Inorg. Chem. **2009**, *48*, 1385−1397

Synthesis and Electrochemical Characterization of Halide, Isocyanide, and Alkynyl Synthons Containing the Encumbered Triangular Cluster Unit $Pt_3(\mu\text{-}P^tBu_2)_3$

Claudia Cavazza,[†] Fabrizia Fabrizi de Biani,[‡] Tiziana Funaioli,[†] Piero Leoni,*[,†] Fabio Marchetti,[†] Lorella Marchetti,[†] and Piero Zanello[‡]

Dipartimento di Chimica e Chimica Industriale, Universita' di Pisa, Via Risorgimento 35, I-56126 Pisa, Italy, and Dipartimento di Chimica dell'Università di Siena, Via A. Moro, I-53100 Siena, Italy

Received July 7, 2008

Useful synthons containing the tribridged triangular unit $\{Pt_3\} = [Pt_3(\mu\text{-}P^tBu_2)_3]^+$ were prepared starting from the known tricarbonyl derivative $[\{Pt_3\}(CO)_3]Z$, [(**1**$^+$)Z, Z = $CF_3SO_3^-$]. This was easily converted into the monohalides $\{Pt_3\}(CO)_2X$ [**2**, X = Cl; **3**, X = Br; **4**, X = I], by reaction with the appropriate halide salt. The coupling reaction between **2** and terminal alkynes in the presence of CuI afforded in good yields the σ-alkynyl derivatives $\{Pt_3\}(CO)_2(CC\text{-}R)$ [**6**, R = $SiMe_3$; **7**, R = CC-$SiMe_3$; **8**, R = C_6H_5; **9**, R = C_6H_4-4-Br; **10**, R = C_6H_4-4-CCH; **11**, R = 2-C_4H_2S-5-CCH; **12**, R = 9-$C_{14}H_8$-10-CCH], while desilylation of **6** or **7** with TBAF/THF gave, respectively, the derivatives **13** (R = H) and **14** (R = CCH). The stepwise elongation of the arylalkynyl chain was obtained by the Sonogashira coupling of **10** with an excess of 1,4-diiodobenzene, which produced **15** (R = C_6H_4-4-CC-C_6H_4-4-I), and by coupling the latter with an excess of 1,4-diethynylbenzene, which formed **16** (R = $[C_6H_4\text{-}4\text{-}CC]_3H$). Branched synthons were obtained by substitution of the carbonyl ligands with functional isocyanides; the reaction of an excess of CN-C_6H_4-4-R (R = I, CCH) with $\{Pt_3\}(CO)_2H$, **5**, or with complex (**1**$^+$)Z afforded, respectively, $\{Pt_3\}(CN\text{-}C_6H_4\text{-}4\text{-}I)_2H$, **17**, or $[\{Pt_3\}(CN\text{-}C_6H_4\text{-}4\text{-}R)_3]Z$ [(**18**$^+$)Z, R = I; (**19**$^+$)Z, R = CCH]. The crystal structures of complexes **2**, **8**, and **9** were established by X-ray diffraction studies. The electrochemical characterization of representative examples of the clusters prepared in this work shows that all clusters are characterized by the presence of two oxidations; an analysis of ligands' effects on the redox processes is also included.

Introduction

The higher stability of M_3 triangles relative to larger M_n rings in transition metal cluster chemistry, recently ascribed to σ-bond aromaticity,[1] is witnessed by the ubiquitous presence of the triangular structural unit. Actually, since the discovery of $Fe_3(CO)_{12}$,[2] thousands of triangular derivatives have been characterized [with more than 4000 structures deposited in the Cambridge Crystallographic Data (CCD) archive][3] thus representing the most common cluster geometry. Clusters of higher nuclearity are generally mostly composed of triangular faces, and indeed, they are in some cases prepared by assembling trinuclear starting materials in different ways, an approach particularly useful for the synthesis of mixed-metal derivatives.[4]

Moreover, a new type of synthetic application has recently been attracting considerable and increasing interest; according to this approach, small metal clusters are used as precursors of large molecular "polycluster" aggregates in which two or

* To whom correspondence should be addressed. E-mail: leoni@dcci.unipi.it.
[†] Universita' di Pisa.
[‡] Dipartimento di Chimica dell'Università di Siena.

(1) King, R. B. *Inorg. Chim. Acta* **2003**, *350*, 126.
(2) Dewar, J.; Jones, H. O. *Proc. R. Soc. London* **1907**, *79A*, 66.
(3) (a) The CSD System. The Cambridge Structural Database: A quarter of a million crystal structures and rising: Allen, F. H. *Acta Crystallogr.* **2002**, *B58*, 380. (b) ConQuest: New software for searching the Cambridge Structural Database and visualizing crystal structures: Bruno, I. J.; Cole, J. C.; Edgington, P. R.; Kessler, M.; Macrae, C. F.; McCabe, P.; Pearson, J.; Taylor, R. *Acta Crystallogr.* **2002**, *B58*, 389.
(4) (a) Underwood, D. J.; Hoffmann, R.; Tatsumi, K.; Nakamura, A.; Yamamoto, Y. *J. Am. Chem. Soc.* **1985**, *107*, 5968. (b) Burrows, A. D.; Mingos, D. M. P. *Coord. Chem. Rev.* **1996**, *154*, 19. (c) Mealli, C. *J. Am. Chem. Soc.* **1985**, *107*, 2245. (d) Imhof, D.; Venanzi, L. M. *Chem. Soc. Rev.* **1994**, 185. (e) Puddephatt, R. J.; Manojlovic-Muir, L.; Muir, K. W. *Polyhedron* **1990**, *9*, 2767. (f) Burrows, A. D.; Mingos, D. M. P. *Coord. Chem. Rev.* **1996**, *154*, 19.

10.1021/ic801268v CCC: $40.75
Published on Web 01/21/2009

more cluster units are not connected by new metal−metal bonds but by firmly bonded organic or organometallic spacers.[5] Although mostly limited (86%) to examples containing only two cluster units, a variety of such structures, assembled from trinuclear precursors (about 300 structures in the CCD file),[3] is now available. Most of them (ca. 85%) contain M_3 units with M = Co,[6] Os,[7] Mo,[8] W,[9] or Ru;[10] quite surprisingly, since Pt_3 clusters are relatively common (ca. 60 structures in the CCD file),[3] only very few Pt_3 polycluster derivatives have been reported until now. To the best of our knowledge, these are limited to the bicluster derivatives $[Pt_3](\mu\text{-}SiMe_2\text{-}R\text{-}Me_2Si)[Pt_3]$ ($[Pt_3] = Pt_3(\mu\text{-}PPh_2)_3(PEt_3)_2$, R = 1,4-diphenylene and 1,1′-ferrocenylene), recently reported by Osakada et al.,[11] to the poorly characterized polymers $[Pt_3(\mu\text{-dppm})_3(CN\text{-}Ar\text{-}NC)]^{2+}$ (Ar = *p*-C_6R_4; R = H, Me)[12] and to the interesting class of derivatives $Pt_6(\mu_2\text{-}CO)_6(\mu_2\text{-}PP)_2(PP)_2$ or $Pt_6(\mu_2\text{-}CO)_6(\mu_2\text{-}PP)_3$ (PP = $Ph_2P\text{-}(CH_2)_n\text{-}PPh_2$, $n = 1-3$) described by Puddephatt et al. in the middle 1990s, which contains two separate triangular $Pt_3(\mu_2\text{-}CO)_3(PP)$ units bridged by two or three PP ligands.[13] Depending upon the length of the bridging diphosphines, these act as encapsulating agents (those containing four PP ligands after dissociation of one chelating diphosphine) for metal centers such as Tl(I) and[13b,c] Hg(0),[13b,c] or when the cage between the two triangles is too small ($n = 1, 2$), they bind Hg(0) or Tl(I) "externally".[13]

A further type of polycluster structure, prepared in our laboratory, is represented by the branched molecule $\{Pt_6\}[(\mu\text{-}CC\text{-}C_6H_3\text{-}(CC\text{-}\{Pt_3\}L_2)_2]_2$, with four triangular units ($\{Pt_3\} = Pt_3(\mu\text{-}P^tBu_2)_3$, L = CO) bonded to a central hexanuclear cluster [$\{Pt_6\} = Pt_6(\mu\text{-}P^tBu_2)_4(CO)_4$] by branched σ-alkynyl spacers,[14a] and by the linear derivative $\{Pt_6\}[(\mu\text{-}CC\text{-}C_6H_4\text{-}CC)(\{Pt_3\}L_2)]_2$.[14b] The structures were assembled starting from the cluster precursors $\{Pt_3\}(CO)_2Cl$ and $\{Pt_6\}Cl_2$, which have a thermally and chemically stable $Pt_x(\mu\text{-}P^tBu_2)_y$ core and a few reactive positions, and, therefore, are particularly suited to be used as cluster synthons. In this paper, we describe a family of new trinuclear derivatives designed as potential building blocks for polycluster molecular assemblies with different types of organic conjugated spacers of different lengths. These mixed valence ($Pt^{I,I,II}$) derivatives share the general formula $[\{Pt_3\}L_{3-n}X_n]^{(1-n)+}$ ($n = 0, 1$; CVE = 44), with the terminal L and X ligands that lie on the molecular plane containing the Pt and P nuclei and are mutually directed at 120°. These features make them interesting potential precursors of clusters containing molecular assemblies. The variable terminal ligands can be three identical π-acceptor neutral molecules; otherwise, one of them can be replaced by a σ-donor, non-π-acceptor, or even π-donor anionic ligand, thus allowing a fine-tuning of the electronic structure. Finally, the electrochemical characterization of representative examples of the clusters prepared in this work has been carried out. In fact, the electron-transfer ability of the building blocks is a fundamental prerequisite to designing the synthesis of a molecular assembly capable of performing useful light- or redox-induced functions. Moreover, the redox propensity of these molecules helps with understanding their electronic structure, and how this can be tuned by the nature of the surrounding ligands. To this purpose, it is noteworthy that only for a couple out of the many triangular platinum cluster reported so far has an electrochemical study been reported. As a matter of fact, we have found that the only reference study about redox behavior concerns the clusters $Pt_3(\mu\text{-}PPh_2)_3(PPh_3)_2Ph$ and $Pt_3(\mu\text{-}PPh_2)_3(PPh_3)_2Si(OMe)_3$, investigated by one of us some years ago.[15]

Results and Discussion

Synthesis of Halides. The neutral monohalides $\{Pt_3\}(CO)_2X$ [$\{Pt_3\} = Pt_3(\mu\text{-}P^tBu_2)_3$; **2**, X = Cl; **3**, X = Br; **4**, X = I] were prepared by adding equimolar amounts of the proper

(5) (a) Humphrey, M. G. *Macromol. Symp.* **2004**, *209*, 1. (b) Notaras, E. G. A.; Lucas, N. T.; Humphrey, M. G.; Willis, A. C.; Rae, A. D. *Organometallics* **2003**, *22*, 3659. (c) Johnson, B. F. G.; Sanderson, K. M.; Shephard, D. S.; Ozkaya, D.; Zhou, W.; Ahmed, H.; Thomas, M. D. R.; Gladden, L.; Mantle, M. *Chem. Commun.* **2000**, 1317. (d) Khairul, W. M.; Porres, L.; Albesa-Jove, D.; Senn, M. S.; Jones, M.; Lydon, D. P.; Howard, J. A. K.; Beeby, A.; Marder, T. B.; Low, P. J. *J. Cluster Sci.* **2006**, *17*, 65.

(6) (a) Calvo-Perez, V.; Shang, M.; Yap, G. P. A.; Rheingold, A.; Fehlner, T. P. *Polyhedron* **1999**, *18*, 1869. (b) Bruce, M. I.; Zaitseva, N. N.; Skelton, B. W. *J. Organomet. Chem.* **2006**, *691*, 759. (c) Bruce, M. I.; Zaitseva, N. N.; Low, P. J.; Skelton, B. W.; White, A. H. *J. Organomet. Chem.* **2006**, *691*, 4273.

(7) (a) Yeh, W.-Y.; Shiue, T. W.; Peng, S.-M.; Lee, G.-H. *Organometallics* **2003**, *22*, 2990. (b) Clarke, L. P.; Cole, J. M.; Davies, J. E.; French, A.; Koentjono, D. F.; Raithby, P. R. *New J. Chem.* **2005**, *29*, 145. (c) Adams, R. D.; Qu, B.; Smith, M. D. *Organometallics* **2002**, *21*, 4847. (d) Ang, S.-G.; Zhong, X.; Ang, H.-G. *Inorg. Chem.* **2002**, *41*, 3791. (e) Lau, J.-P. K.; Wong, W. T. *Inorg. Chim. Acta* **2006**, *369*, 3632.

(8) (a) Tang, Y.-H.; Qin, Y.-Y.; Li, Z.-J.; Zang, J.; Kang, Y.; Hu, R.-F.; Wen, Y.-H.; Cheng, J.-K.; Yao, Y.-G. *Bull. Chem. Soc. Jpn.* **2005**, *78*, 626. (b) Sakane, G.; Kawasaki, H.; Oomori, T.; Yamasaki, M.; Adachi, H.; Shibahara, T. *J. Cluster Sci.* **2002**, *13*, 75. (c) Fedin, V. P.; Sokolov, M.; Lamprecht, G. J.; Hernandez-Molina, R.; Seo, M.-S.; Virovets, A. V.; Clegg, W.; Sykes, A. G. *Inorg. Chem.* **2001**, *40*, 6598. (d) Yu, R.-M.; Lu, S.-F.; Huang, X.-Y.; Wu, Q. J.; Huang, J.-Q. *Inorg. Chem.* **1999**, *38*, 3313.

(9) (a) Sin, S.; Di Salvo, F. *J. Chem. Mater.* **2002**, *14*, 3448. (b) Yu, S.-B.; Droege, M.; Downey, S.; Segal, B.; Newcomb, W.; Sanderson, T.; Crofts, S.; Suravajjala, S.; Bacon, E.; Earley, W.; Delecki, D.; Watson, A. D. *Inorg. Chem.* **2001**, *40*, 1576. (c) Almond, M. J.; Drew, M. G. B.; Redman, H.; Rice, D. A. *Polyhedron* **2000**, *19*, 2127. (d) Sokolov, M. N.; Virovets, A. V.; Dybtsev, D. N.; Gerasko, O. A.; Fedin, V. P.; Hernandez-Molina, R.; Clegg, W.; Sykes, A. G. *Angew. Chem., Int. Ed.* **2000**, *39*, 1659.

(10) (a) Bruce, M. I.; Humphrey, P. A.; Melino, G.; Skelton, B. W.; White, A. H.; Zaitseva, N. N. *Inorg. Chim. Acta* **2005**, *358*, 1453. (b) O'Connor, A. R.; Nataro, C.; Rheingold, A. L. *J. Organomet. Chem.* **2003**, *679*, 72. (c) Hanif, K. M.; Kabir, S. E.; Mottalib, M. A.; Hursthouse, M. B.; Malik, K. M. A.; Risenberg, E. *Polyhedron* **2000**, *19*, 1073. (d) Dorta, R.; Stoeckli-Evans, H.; Bodensieck, U.; Suss-Fink, G. *J. Organomet. Chem.* **1998**, *553*, 307. (e) Van Calcar, P. M.; Olmstead, M. M.; Balch, A. L. *Inorg. Chim. Acta* **1998**, *270*, 28.

(11) Izataki, M.; Kitami, O.; Tanabe, M.; Nishihara, Y.; Osakada, K. *J. Organomet. Chem.* **2005**, *690*, 3957.

(12) Bradford, A. M.; Kristof, E.; Rashidi, M.; Yang, D. S.; Payne, N. C.; Puddephatt, R. J. *Inorg. Chem.* **1994**, *33*, 2355.

(13) (a) Hao, L.; Spivak, G. J.; Xiao, J.; Vittal, J. J.; Puddephatt, R. J. *J. Am. Chem. Soc.* **1995**, *117*, 7011. (b) Hao, L.; Vittal, J. J.; Puddephatt, R. J. *Organometallics* **1996**, *15*, 3115. (c) Hao, L.; Vittal, J. J.; Puddephatt, R. J. *Inorg. Chem.* **1996**, *35*, 269.

(14) (a) Albinati, A.; Leoni, P.; Marchetti, L.; Rizzato, S. *Angew. Chem., Int. Ed.* **2003**, *42*, 5990. (b) Leoni, P.; Marchetti, F.; Marchetti, L.; Pasquali, M. *Chem. Commun.* **2003**, 2372. (c) Leoni, P.; Marchetti, L.; Mohapatra, S. K.; Ruggeri, G.; Ricci, L. *Organometallics* **2006**, *25*, 4226. (d) Fabrizi de Biani, F.; Ienco, A.; Laschi, F.; Leoni, P.; Marchetti, F.; Marchetti, L.; Mealli, C.; Zanello, P. *J. Am. Chem. Soc.* **2005**, *127*, 3076.

(15) Bender, R.; Braunstein, P.; Bouaoud, S.-E.; Merabet, N.; Rouag, D.; Zanello, P.; Fontani, M. *New J. Chem.* **1999**, *23*, 1045.

Scheme 1

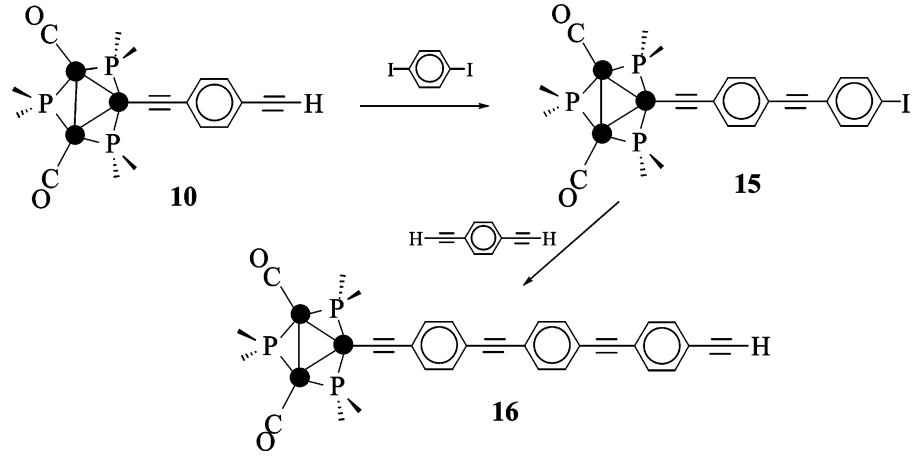

t-butylammonium halide to an acetone solution of the symmetrical (D_{3h}) monocationic tricarbonyl derivative [{Pt_3}-$(CO)_3$]Z, ($\mathbf{1}^+$)Z (Z = $CF_3SO_3^-$).[14d]

After stirring for a few hours at room temperature, complexes **2**−**4** may be isolated in good yields (>92%) and remain unchanged even after prolonged reaction times under a large molar excess of the halide. Crystalline brown solids, and single crystals for **2**, were obtained by recrystallization from acetone. As compared to cation $\mathbf{1}^+$ (ν_{CO} = 2064 cm^{-1}), the IR carbonyl stretching absorption is shifted to ca. 2030 cm^{-1}, as expected after substitution of a π-acceptor carbonyl with the σ-donor halide and the resulting charge reduction. The chloride derivative **2** proved to be a better precursor than **3** or **4** (faster reactions) for the corresponding alkynyl complexes **6**−**12**, which were obtained by the CuI (1%) catalyzed dehydrohalogenation occurring in the reactions of **2** with equimolar amounts of the appropriate terminal alkyne in amine solvents. The reactions must be performed under a rigorously inert atmosphere to avoid self-coupling of the ethynyl function and give the desired products as brown solids [76−90% (isolated) yields], which exhibit significant IR absorptions at ca. 2020 (ν_{CO}), 2100 (ν_{CC}), and 3100 ($\nu_{CC\text{-}H}$) cm^{-1}, as expected by comparison with the corresponding absorptions of **2**−**4** and of the numerous known mononuclear alkynyl complexes.[16] Complex **6** was also prepared by reacting Me_3Si-CCLi with complex **2** in THF. Single crystals of **8** and **9** suitable for crystallographic studies were grown by slow evaporation of chloroform solutions.

Clean deprotection of the trimethylsilyl derivatives **6** and **7** to afford, respectively, the ethynyl and butadiynyl complexes **13** (70%) and **14** (78%) was obtained by reaction with tetrabutylammonium fluoride (TBAF, equimolar) in THF. Indeed, **7** can also be deprotected with K_2CO_3 in MeOH, with NaOH, or with KF in MeOH/THF, while under the same conditions, complex **6** remained unchanged. The ethynyl and butadiynyl complexes **13** and **14** were also prepared (80% yield) directly by dehydrohalogenation from **2** and acetylene or butadiyne, respectively. The length of the arylalkynyl ligands may be changed at will, for example, by following the stepwise procedure shown in Scheme 1. According to this procedure, complex **10** was first reacted with an excess of 1,4-diiodobenzene, to afford **15**, which was then reacted with an excess of 1,4-diethynylbenzene to give **16**; these contain two or three −CC-C_6H_4− units and may be considered as useful precursors of polycluster structures with spacers of variable length. Both reactions were performed in $NHEt_2$ in the presence of CuI (1%) and $Pd(PPh_3)_2Cl_2$ (1%) catalysts, and **15** (65%) and **16** (62%) were isolated as green-brown solids.

The terminal carbonyls of this series of derivatives may be easily and cleanly exchanged with other neutral 2 e^- donors. Clusters with two or three spacer precursors, lying on the Pt_3P_3 molecular plane and mutually directed at 120°, may therefore be prepared. These derivatives are useful potential precursors of cluster-containing zigzag chains or of planar networks with size-adjustable cavities. For example, the known hydride[17] {Pt_3}$(CO)_2$H reacts with an excess of *p*-iodophenylisocyanide to give cleanly {Pt_3}(CN-C_6H_4-4-I))$_2$H (**17**) as an orange solid (75%). Moreover, symmetrical tris-isocyanide derivatives were prepared by reacting the tricarbonyl complex ($\mathbf{1}^+$)Z with a slight excess of *p*-iodophenylisocyanide or *p*-ethynylphenylisocyanide to afford [{Pt_3}(CN-C_6H_4-4-R)$_3$]Z [($\mathbf{18}^+$)Z, R = I, 92%; ($\mathbf{19}^+$)Z, R = CCH, 94%] as green solids. Satisfactory microanalytical data and pertinent IR and NMR spectroscopical features were obtained for all complexes (see Table 1 and Experimental Section).

NMR Spectra. All NMR spectra arise from the sum of subspectra due to the eight isotopomers **A**−**H** with different content of the NMR-active ^{195}Pt nucleus (I = 1/2, NA =

(16) (a) Manojlovic-Muir, L.; Muir, K. W.; Treurnicht, I.; Puddephatt, R. J. *Inorg. Chem.* **1987**, *26*, 2418. (b) Baralt, E.; Boudreaux, E. A.; Demas, J. N.; Lenhert, P. G.; Lukehart, C. M.; McPhail, A. T.; McPhail, D. R.; Myers, J. B., Jr.; Sacksteder, L.; True, W. R. *Organometallics* **1989**, *8*, 2417. (c) Yam, V. W.-W.; Wong, K. M.-C.; Zhu, N. *J. Am. Chem. Soc.* **2002**, *124*, 6506. (d) Yip, J. H. K.; Wu, J.; Wong, K.-Y.; Ho, K. P.; Pun, C. S.-N.; Vittal, J. J. *Organometallics* **2002**, *21*, 5292. (e) Ciriano, M.; Howard, J. A. K.; Spencer, J. L.; Stone, F. G. A.; Wadepohl, H. *J. Chem. Soc., Dalton Trans.* **1979**, 1749.

(17) Leoni, P.; Manetti, S.; Pasquali, M.; Albinati, A. *Inorg. Chem.* **1996**, *35*, 6045.

Table 1. Selected NMR Parameters for Complexes **1**−**19**

Isotop	Pt_1	Pt_2	Pt_3	%	Spin System
A	-	-	-	29.0	A_2M
B	^{195}Pt	-	-	14.8	AA'MX
C	-	^{195}Pt	-	14.8	AA'MX
D	-	-	^{195}Pt	14.8	A_2MX
E	^{195}Pt	^{195}Pt	-	7.6	AA'MXX'
F	^{195}Pt	-	^{195}Pt	7.6	AA'MXY
G	-	^{195}Pt	^{195}Pt	7.6	AA'MXY
H	^{195}Pt	^{195}Pt	^{195}Pt	4.8	AA'MXX'Y

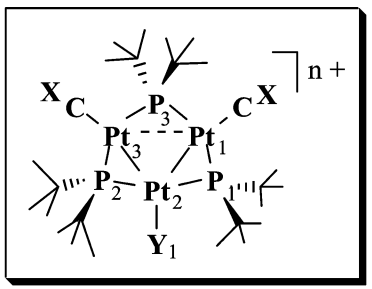

Compl	X	Y	n
1	CO	CO	1
2	CO	Cl	0
3	CO	Br	0
4	CO	I	0
5	CO	H	0
6	CO	CC-TMS	0
7	CO	CC-CC-TMS	0
8	CO	CC-Ph	0
9	CO	CC-C_6H_4-Br	0
10	CO	CC-C_6H_4-CCH	0
11	CO	CC-C_4H_2S-CCH	0
12	CO	CC-$C_{14}H_8$-CCH	0
13	CO	CCH	0
14	CO	CC-CCH	0
15	CO	$(CC\text{-}C_6H_4)_2$-I	0
16	CO	$(CC\text{-}C_6H_4)_3$-CCH	0
17	CN-C_6H_4-I	H	0
18	CN-C_6H_4-I	CN-C_6H_4-I	1
19	CN-C_6H_4-CCH	CN-C_6H_4-CCH	1

	1	**2**	**3**	**4**	**5**	**6**	**7**	**8**	**9**	**10**	**11**	**12**	**13**	**14**	**15**	**16**	**17**	**18**	**19**
$\delta_{P1,2}$	154.6	167.8	168.8	171.8	220.9	163.7	159.1	165.3	168.2	164.7	162.2	164.3	161.4	161.3	164.5	162.8	203.3	140.0	140.1
δ_{P_3}	154.6	46.7	50.9	64.6	99.2	98.8	108.4	96.4	92.3	98.6	102.5	101.9	101.8	104.4	103.1	101.0	99.1	140.0	140.1
$\delta_{Pt_{1,3}}$	5950	5320	5345	5472	5611	5709	5774	5723	5735	5722	5738	-5737	-5747	-5754	-5724	-5767	-5599	-5973	-5980
δ_{Pt_2}	5950	6390	6611	6928	6893	6088	6033	6088	6178	6085	6071	-6063	-6066	-6072	-6082	-6105	-6916	-5973	-5980
$^2J_{P_1P_3}$, $^2J_{P_2P_3}$	130	130	128	124	152	127	126	128	129	128	128	127	126	126	128	125	163	158	158
$^2J_{P_1P_2}$	130	246	236	245	164	239	226	239	230	234	226	230	240	230	235	232	189	158	158
$^1J_{Pt_1P_3}$, $^1J_{Pt_3P_3}$	1786	1709	1706	1711	2064	1829	1814	1822	1832	1831	1820	1822	1817	1814	1821	1819	2102	1939	1932
$^1J_{Pt_1P_1}$, $^1J_{Pt_3P_2}$	1786	1944	1942	1850	2541	1880	1828	1877	1922	1872	1859	1843	1838	1828	1881	1889	2399	1939	1932
$^1J_{Pt_2P_1}$, $^1J_{Pt_2P_2}$	1786	2233	2226	2214	2022	2125	2124	2132	2130	2125	2114	2120	1987	2102	2124	2127	2142	1939	1932
$^2J_{Pt_2P_3}$	-100	-152	-154	-152	-253	-105	-90	-98	-105	-99	-99	-100	-95	-93	-102	-99	-206	-101	-96
$^2J_{Pt_1P_2}$, $^2J_{Pt_3P_1}$	-100	-30	-38	-52	-116	-55	-75	-56	-56	-56	-52	-56	-68	-73	-64	-72	-39	-101	-96
$^1J_{Pt_1Pt_3}$	1800	1270	1288	1407	650	1850	2000	1912	1755	1926	1900	1845	1987	2000	2083	2073	528	1506	1470
$^1J_{Pt_1Pt_2}$, $^1J_{Pt_3Pt_2}$	1800	2026	2190	2257	780	877	942	926	928	941	957	926	926	962	934	893	683	1506	1470

33.8%); the numbering scheme and the composition, relative abundance, and spin systems of the various isotopomers are given in Table 1.

The $^{31}P\{^1H\}$ NMR spectra of the neutral complexes **2**−**17** consist of a signal in the low-field region from 159 to 221 ppm for the equivalent nuclei P(1) and P(2), well separated from another signal, assigned to P(3) (46−109 ppm). Two signals were observed also in the $^{195}Pt\{^1H\}$ NMR spectra [between −5320 and −5780 ppm for the equivalent nuclei Pt(1) and Pt(3), and between −6030 and −6930 ppm for Pt(2)]. Some of the coupling constants shown in Table 1 [$^2J_{P1P3} = {}^2J_{P2P3}$, $^1J_{Pt1P3} = {}^1J_{Pt3P3}$, $^2J_{Pt2P3}$, $^1J_{Pt2P1} = {}^1J_{Pt2P2}$, and $^1J_{Pt1Pt2} = {}^1J_{Pt3Pt2}$] can be straightforwardly achieved from the first-order signals of P(3) and Pt(2); the remaining ones can be accurately determined through simulation,[18a] which reproduces nicely the complex pattern of the higher-order satellites of the signals of P(1,2) and Pt(1,3).[18b]

The shifts of the signals observed upon changing the terminal anionic ligand Y (Table 1) deserve some comment. The values of δ_{Pt} are spread in relatively narrow ranges: as compared to the mean value of the intervals given above, $\delta_{Pt1,3}$ varies by only ca. ±8%, and the shifts of the platinum nucleus directly bonded to Y, δ_{Pt2}, vary by ca. ±14%. Phosphorus chemical shifts are much more erratic, and the distribution of the values of $\delta_{P1,2}$ and δ_{P3} reaches, respectively, ±32% (but less than ±8% if the highly deshielded signals of the hydrides **5** and **17** are excluded) and ±80% (**5** and **17** included) of the corresponding mean value. Moreover, by registering the spectra of complex **2** in acetone-d_6, $CDCl_3$, Et_2O-d_{10}, or C_6D_6, while all other parameters vary in narrow ranges, δ_{P3} is observed at 54.2, 46.7, 43.0, and 42.3, respectively. It is noteworthy that, also, the *direction* of the shift is in some case unusual; indeed, δ_{P3} moves progressively to a high field upon increasing the halide electronegativity, opposite of what is generally observed in mononuclear $(R_3P)_xMX_y$ derivatives.[19] Although less pronounced, the same trend was observed for the values of $\delta_{P1,2}$, while the inverse drift is exhibited by those of δ_{Pt}. In addition to charge redistribution occurring upon substitution at Pt_2, other effects may have an influence on these intriguing trends. In fact, it is well-known that δ_P shifts of bridging phosphides span a very broad range, from very low fields (up to 450 ppm), typical of bridges on a metal−metal bonded edge, to the opposite upfield region (up to −150 ppm), when the metal−metal bond is absent.[20a] On the other hand, it is now well recognized that the Pt−Pt bond opposite the anionic ligand Y [Pt(1)−Pt(3) in **2**−**17**] in the $Pt_3(\mu\text{-}PR_2)_3L_2Y$ series of clusters has a very soft deformation potential. This is witnessed by the skeletal isomerism observed in $Pt_3(\mu\text{-}PPh_2)_3(PPh_3)_2(Ph)$ (**20**),[20] which crystallizes from toluene−pentane, forming an isosceles triangle with two short Pt(2)−Pt(1,3) [2.758(3) Å] and one long Pt(1)−Pt(3) [3.586(2) Å] bond. When crystallization occurs from a CH_2Cl_2−pentane mixture, **20** forms a quasi-equilateral triangle [Pt(2)−Pt(1,3) = 2.956(3); Pt(1)−Pt(3) = 3.074(4) Å]. In addition, we found that complex **5** crystallizes in the "isosceles" fashion [molecule A: Pt(2)−Pt(1,3) = 2.7165(6), 2.7247(6); Pt(1)−Pt(3) = 3.6135(6) Å; molecule B: Pt(2)−Pt(1,3) = 2.7196(6), 2.7246(6); Pt(1)−Pt(3) = 3.6249(6) Å],[17] while its isocyanide analogue $Pt_3(\mu\text{-}P^tBu_2)_3(CN^tBu)_2H$[21] has an "equilateral", temperature-sensitive, structure [Pt(2)−Pt(1,3) = 2.9014(8), 2.9145(7); Pt(1)−Pt(3) = 3.1709(8) Å at 298 K and Pt(2)−Pt(1,3) = 2.9624(3), 2.9485(3); Pt(1)−Pt(3) = 3.0906(3) Å at 200 K]. Finally, in the branched derivative $\{Pt_6\}[(\mu\text{-}CC\text{-}C_6H_3\text{-}(CC-\{Pt_3\}L_2)_2]_2$,[14a] the four identical triangular units exhibit four different Pt(1)−Pt(3) distances spread in a broad range between 3.066 and 3.380 Å. It is well evident that the length of the Pt(1)−Pt(3) bond can vary between ca. 2.9 and 3.6 Å without significantly modifying the stability of the complex. Indeed, a theoretical study[20a] has shown that, when Y is a σ-donor ligand, the "open" and "closed" forms differ in energy by only a few kilocalories per mole. Therefore, the Pt(1)−Pt(3) bond distance is markedly influenced, much more than other bond distances, by relatively small enthalpic contributions such as packing forces in the solid state or solvent effects in solution, and by the temperature. It is also worth mentioning that, according to the same theoretical analysis,[20a] when Y is a neutral π-acceptor ligand, the open isosceles structure becomes unstable; indeed, the two crystallographically characterized $[Pt_3(\mu\text{-}PR_2)L_2L']^+$ cations[14d,21] (R = ^{t}Bu, L = CO, L′ = CO, CH_2CH_2) crystallize in the equilateral form, with all Pt−Pt bond lengths varying in the narrow range between 2.91 and 3.03 Å. Accordingly, they exhibit downfield-shifted values of δ_{P3} (154.6 and 166.6 ppm, respectively).

The ^1H and $^{13}C\{^1H\}$ NMR spectra of all complexes show signals with the expected frequencies, coupling constants, and intensities and are in full agreement with the structures proposed in Table 1.

Crystal and Molecular Structures of 2, 8, and 9. A projection of the molecular structure of **2** is shown in Figure 1, and a selection of the bond distances and angles is listed in Table 2.

The molecule exhibits an isosceles Pt_3 core, with two short Pt(1)−Pt(2) [2.853(1) Å] and one long Pt(2)−Pt(2′) [3.152(1) Å] distance. The latter is situated within the very broad range (2.9−3.65 Å) previously found for the Pt−Pt distance opposing the X ligand in other $Pt_3(\mu\text{-}PR_2)_3L_2X$ complexes

(18) (a) Spectral parameters were determined iteratively using full lineshape analysis with the computer program gNMR: P. H. M. Budzelaar, gNMR, version 5.0.6.0, 2006. (b) A more detailed description of the $^{31}P\{^1H\}$ and $^{195}Pt\{^1H\}$ NMR signals observed for complex **5** and figures showing its experimental and simulated spectra may be found in ref 17.

(19) (a) Mann, B. E.; Masters, C.; Shaw, B. L. *J. Chem. Soc., Dalton Trans.* **1972**, 704. (b) Garrou, P. E.; Hartwell, G. E. *Inorg. Chem.* **1976**, *15*, 646. (c) Hyde, E. M.; Kennedy, J. D.; Shaw, B. L.; McFarlane, W. *J. Chem. Soc., Dalton Trans.* **1977**, 1571. (d) MacDougall, J. J.; Nelson, J. H.; Mathey, F. *Inorg. Chem.* **1982**, *21*, 2145. (e) Rahn, J. A.; O'Donnell, D. J.; Palmer, A. R.; Nelson, J. H. *Inorg. Chem.* **1989**, *28*, 2631. (f) Grim, S. O.; Lui, P. J.; Keiter, R. L. *Inorg. Chem.* **1974**, *13*, 342. (g) Alyea, E. C.; Dias, S. A.; Goel, R. G.; Ogini, W. O.; Pilon, P.; Meek, D. W. *Inorg. Chem.* **1978**, *17*, 1697.

(20) (a) Bender, R.; Braunstein, P.; Dedieu, A.; Ellis, P. D.; Huggins, B.; Harvey, P. D.; Sappa, E.; Tiripicchio, A. *Inorg. Chem.* **1996**, *35*, 1223. (b) Bender, R.; Braunstein, P.; Tiripicchio, A.; Tiripicchio Camellini, M. *Angew. Chem., Int. Ed. Engl.* **1985**, *24*, 861.

(21) Leoni, P.; Marchetti, F.; Pasquali, M.; Marchetti, L.; Albinati, A. *Organometallics* **2002**, *21*, 2176.

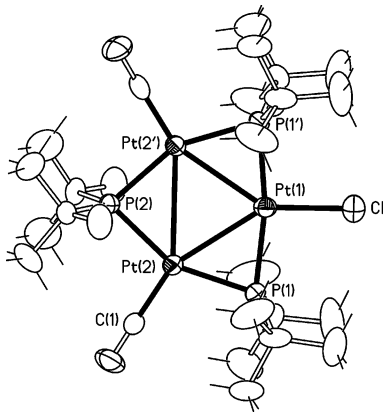

Figure 1. View of the molecular structure of **2**. Thermal ellipsoids are at 30% probability. The $' = x, 1/2 - y, z$.

Table 2. Bond Lengths [Å] and Angles [deg] around Pt Atoms in **2**

Pt(1)−Pt(2)	2.853(1)	Pt(2)−Pt(2′)	3.152(1)
Pt(1)−P(1)	2.274(5)	Pt(1)−Cl	2.31(1)
Pt(2)−P(1)	2.283(5)	Pt(2)−P(2)	2.313(6)
Pt(2)−C(1)	1.85(2)		
P(1′)−Pt(1)−P(1)	169.8(3)	P(1)−Pt(1)−Cl	95.1(1)
P(1)−Pt(1)−Pt(2)	51.4(1)	Cl−Pt(1)−Pt(2)	146.4(2)
P(1)−Pt(1)−Pt(2′)	118.5(1)	Pt(2)−Pt(1)−Pt(2′)	67.1(4)
C(1)−Pt(2)−P(1)	105.0(6)	C(1)−Pt(2)−P(2)	100.4(6)
P(1)−Pt(2)−P(2)	154.6(2)	C(1)−Pt(2)−Pt(1)	156.0(6)
P(1)−Pt(2)−Pt(1)	51.1(1)	P(2)−Pt(2)−Pt(1)	103.5(1)
C(1)−Pt(2)−Pt(2′)	147.2(6)	P(1)−Pt(2)−Pt(2′)	107.6(1)
P(2)−Pt(2)−Pt(2′)	47.0(1)	Pt(1)−Pt(2)−Pt(2′)	56.5(2)

(see above)[20,21] and, although rather long, is still shorter than the sum of Pt van der Waals radii (3.4 Å).[22] The phosphorus and chlorine atoms and the CO ligands approximately lie on the Pt_3 plane [maximum deviation 0.109 Å for C(1)], simulating an *m*2*m* (C_{2v}) symmetry.

Each pair of *t*-butyl groups lies on either side of the Pt_3 plane, thus offering steric protection to the inner $Pt_3(\mu\text{-}P)_3$ core. The Pt−P distances, between 2.27 and 2.31 Å, are in the expected range of previously determined $\{Pt_3\}(CO)_2X$ structures.[14a,17,21] The Pt(1)−Cl bond length in **2** [2.31(1) Å] is considerably shorter than in $[Pt_3(\mu_2\text{-dppm})_3(\mu_3\text{-CO})Cl]Cl$ [2.785(8) Å],[23a] where, however, the Pt−Cl interaction is very weak (the distance is almost 0.5 Å longer than the sum of the covalent radii) due to the steric encumbrance of the phenyl groups of the dppm ligands. It is also shorter than in the other unique example of a platinum cluster containing a terminal Pt−Cl bond, namely, $Pt_4(\mu_3\text{-O})_2Cl_2(dmso)_6$ [Pt−Cl = 2.439−2.473 Å];[23b] in this derivative, the relatively long Pt−Cl distance may be attributed to the high trans influence of the Pt−Pt bond [Pt−Pt−Cl = 167.60−171.61°]. Dinuclear or linear polynuclear derivatives with terminal Pt−Cl ligands are relatively common[24] and exhibit Pt−Cl distances in the range 2.27−2.5 Å, with Pt−Cl bonds trans to Pt−Pt bonds quite generally above 2.38 Å, and those trans to all other ligands quite generally below the same threshold. The molecular structure of **8** is shown in Figure 2, and its more significant geometrical parameters are listed in Table 3.

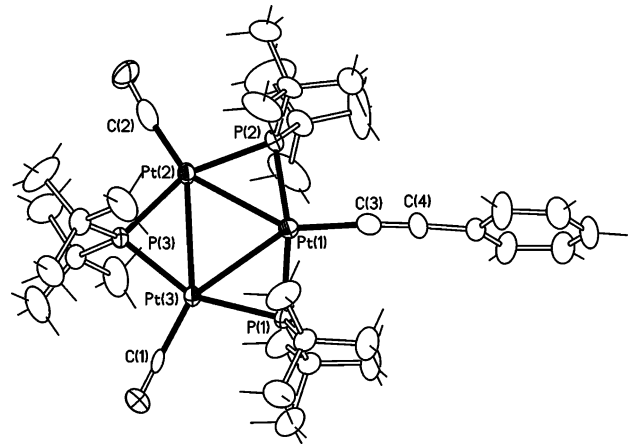

Figure 2. View of the molecular structure of **8**. Thermal ellipsoids are at 30% probability.

Table 3. Bond Lengths [Å] and Angles [deg] around Pt Atoms in **8**

Pt(1)−C(3)	1.96(1)	Pt(2)−P(2)	2.302(3)
Pt(1)−P(1)	2.259(3)	Pt(2)−P(3)	2.310(3)
Pt(1)−P(2)	2.263(3)	Pt(2)−Pt(3)	3.1181(7)
Pt(1)−Pt(2)	2.8908(8)	Pt(3)−C(1)	1.82(1)
Pt(1)−Pt(3)	2.9045(7)	Pt(3)−P(1)	2.296(3)
Pt(2)−C(2)	1.86(2)	Pt(3)−P(3)	2.303(3)
C(3)−Pt(1)−P(2)	97.9(4)	P(3)−Pt(2)−Pt(1)	104.90(8)
C(3)−Pt(1)−P(1)	94.8(4)	C(2)−Pt(2)−Pt(3)	151.7(4)
P(2)−Pt(1)−P(1)	166.6(1)	P(2)−Pt(2)−Pt(3)	107.77(8)
C(3)−Pt(1)−Pt(2)	149.2(4)	P(3)−Pt(2)−Pt(3)	47.38(7)
P(2)−Pt(1)−Pt(2)	51.31(7)	Pt(1)−Pt(2)−Pt(3)	57.66(2)
P(1)−Pt(1)−Pt(2)	115.90(7)	C(1)−Pt(3)−P(1)	103.0(5)
C(3)−Pt(1)−Pt(3)	145.7(4)	C(1)−Pt(3)−P(3)	102.6(5)
P(2)−Pt(1)−Pt(3)	116.41(7)	P(1)−Pt(3)−P(3)	154.5(1)
P(1)−Pt(1)−Pt(3)	50.95(7)	C(1)−Pt(3)−Pt(1)	152.8(4)
Pt(2)−Pt(1)−Pt(3)	65.10(2)	P(1)−Pt(3)−Pt(1)	49.82(8)
C(2)−Pt(2)−P(2)	100.5(4)	P(3)−Pt(3)−Pt(1)	104.66(7)
C(2)−Pt(2)−P(3)	104.5(4)	C(1)−Pt(3)−Pt(2)	150.0(5)
P(2)−Pt(2)−P(3)	154.9(1)	P(1)−Pt(3)−Pt(2)	106.92(8)
C(2)−Pt(2)−Pt(1)	150.6(4)	P(3)−Pt(3)−Pt(2)	47.57(7)
P(2)−Pt(2)−Pt(1)	50.11(8)	Pt(1)−Pt(3)−Pt(2)	57.24(2)

Complex **8** contains the same roughly planar core present in **2**, with the isosceles Pt_3 triangle having approximately the same bond lengths. In this case, however, the molecule in the crystal does not adopt the mirror perpendicular to the platinum triangle, resulting in complete asymmetry. This is due to the phenyl plane of the alkynyl ligand, which makes an angle of 82.3° with the Pt_3 plane, probably complying with the steric requirements of the packing. The Pt(1)−C(3), 1.96(1) Å, and C(3)−C(4), 1.21(2) Å, bond lengths fall in the range commonly found for terminal phenylacetylide ligands bonded to platinum.[16]

(22) (a) Bondi, A. *J. Phys. Chem.* **1964**, *68*, 441. (b) Bondi, A. *Physical Properties of Molecular Crystals, Liquids and Glasses*; Wiley: New York, 1968.

(23) (a) Holah, D. G.; Hughes, A. N.; Krysa, E.; Spivak, G. J.; Havighurst, M. D.; Magnuson, V. R. *Polyhedron* **1997**, *11*, 2353. (b) Betz, P.; Bino, A. *J. Am. Chem. Soc.* **1988**, *110*, 602.

(24) Selected examples: (a) Matsumoto, K.; Arai, S.; Ochiai, M.; Chen, W.; Nakata, A.; Nakai, H.; Kinoshita, S. *Inorg. Chem.* **2005**, *44*, 8552. (b) Sakai, K.; Tanaka, Y.; Tsuchiya, Y.; Hirata, K.; Tsubomura, T.; Iijima, S.; Bhattacharjee, A. *J. Am. Chem. Soc.* **1998**, *120*, 8366. (c) Arena, C. G.; Ciani, G.; Drommi, D.; Faraone, F.; Prosperpio, D. M.; Rotondo, E. *J. Organomet. Chem.* **1994**, *484*, 71. (d) Tanase, T.; Ukaji, H.; Igoshi, T.; Yamamoto, Y. *Inorg. Chem.* **1996**, *35*, 4114. (e) Micklitz, W.; Renn, O.; Schollborn, H.; Thewalt, U.; Lippert, B. *Inorg. Chem.* **1990**, *29*, 1836. (f) Poater, A.; Moradell, S.; Pinilla, E.; Poater, J.; Sola, M.; Martinez, M. A.; Llobet, A. *Dalton Trans.* **2006**, 1188. (g) Umakoshi, K.; Sasaki, Y. *Inorg. Chem.* **1997**, *36*, 4296. (h) Cini, R.; Donati, A.; Giannettoni, R. *Inorg. Chim. Acta* **2001**, *315*, 73. (i) Liu, F.; Chen, W.; Wang, D. *Dalton Trans.* **2006**, 3445.

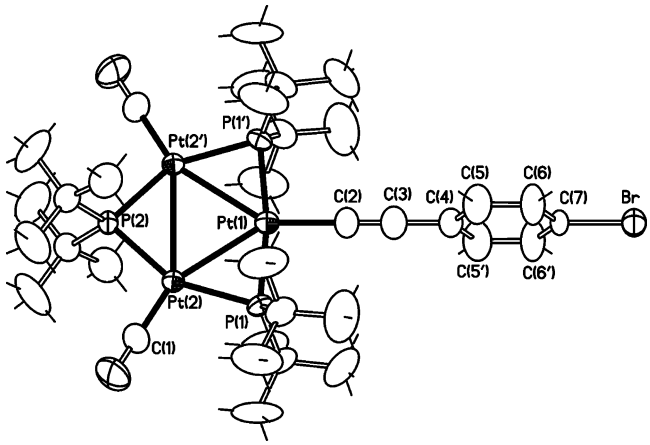

Figure 3. View of the molecular structure of **9**. Thermal ellipsoids are at 30% probability. The $' = -x, y, 1/2 - z$.

Table 4. Bond Lengths [Å] and Angles [deg] around Pt Atoms in **9**

Pt(1)−Pt(2)	2.8558(8)	Pt(2)−Pt(2′)	3.204(1)
Pt(1)−P(1)	2.272(3)	Pt(1)−C(2)	2.01(2)
Pt(2)−P(1)	2.280(3)	Pt(2)−P(2)	2.296(3)
Pt(2)−C(1)	1.82(2)		
C(2)−Pt(1)−P(1)	94.62(9)	P(1)−Pt(1)−Pt(2)	51.26(9)
P(1)−Pt(1)−P(1′)	170.8(2)	P(1)−Pt(1)−Pt(2′)	119.50(9)
C(2)−Pt(1)−Pt(2)	145.88(1)	Pt(2)−Pt(1)−Pt(2′)	68.24(3)
C(1)−Pt(2)−P(1)	104.0(6)	P(2)−Pt(2)−Pt(1)	101.65(8)
C(1)−Pt(2)−P(2)	103.4(6)	C(1)−Pt(2)−Pt(2′)	149.1(6)
P(1)−Pt(2)−P(2)	152.7(1)	P(1)−Pt(2)−Pt(2′)	106.91(9)
C(1)−Pt(2)−Pt(1)	155.0(6)	P(2)−Pt(2)−Pt(2′)	45.77(7)
P(1)−Pt(2)−Pt(1)	51.03(9)	Pt(1)−Pt(2)−Pt(2′)	55.88(1)

Table 5. Formal Electrode Potentials (V vs SCE; and Peak-to-Peak Separations, in mV), in CH_2Cl_2 Solution for the Redox Processes Exhibited by $[\{Pt_3\}L_{3-n}X_n]^{(1-n)+}$

	oxidation processes				reduction processes	
complex	$E^{\circ\prime}$	ΔE_p[a]	$E^{\circ\prime}$	ΔE_p[a]	$E^{\circ\prime}$	ΔE_p[a]
1$^+$	+1.56		+1.13	*90*	−1.29[b]	
2	+0.91	*70*	+0.31	*60*	−1.91[c]	
3	+0.88	*70*	+0.29	*60*	−1.91[c]	
4	+0.86	*70*	+0.28	*70*	−1.91[c]	
5	+0.70[b]	*75*	+0.26	*80*		
6	+0.63[b]		+0.26	*70*		
8	+0.75[c]		+0.30	*85*		
10	+0.95[c]		+0.31	*85*		
18$^+$	+0.90[b]	*100*	+0.44	*100*	−1.24[b]	*80*
19$^+$	+0.92	*60*	+0.45	*58*	−1.67[c]	

[a] Measured at 0.2 V s^{-1}. [b] Coupled to relatively fast chemical reactions. [c] Coupled to fast chemical reactions.

Figure 3 shows a projection of the structure of compound **9**; relevant bond distances and angles are listed in Table 4.

This molecule crystallizes in the orthorhombic *Cmcm* space group adopting in the crystal its maximum symmetry *m*2*m* (C_{2v}) so that the asymmetric unit is only a quarter of the molecule. The bromophenylacetylide ligand is aligned with the 2-fold axis of the molecule, with the phenyl plane perpendicular to the Pt_3 triangle. The bond geometry of the ethynyl group is not significantly different from the one observed in **8**.

Electrochemistry. The electrochemical investigation of the 44 e$^-$ $[\{Pt_3\}L_{3-n}X_n]^{(1-n)+}$ clusters is expected to gather interesting information about the influence of the nature of the ligands L and X on their stability. Table 5 compiles the formal electrode potentials of the redox changes observed for these compounds. In CH_2Cl_2 solution, all compounds undergo two sequential monoelectronic oxidations, which substantially typify their redox fingerprint. In passing, we may notice that the previously studied $Pt_3(\mu\text{-}PPh_2)_3(PPh_3)_2Ph$ and $Pt_3(\mu\text{-}PPh_2)_3(PPh_3)_2Si(OMe)_3$, which also have 44 valence electrons, similarly undergo the removal of two electrons (in one and two single steps for the former and the latter, respectively).[15] Being the formal parent of this family of clusters, $[\{Pt_3\}(CO)_3]^+$, **1**$^+$, will be discussed first. This compound undergoes two monoelectronic oxidations (at +1.13 and +1.56 V). Only the first oxidation is chemically reversible on the time scale of the cyclic voltammetry, whereas the second oxidation is complicated by a subsequent chemical reaction. A single irreversible reduction process at −1.29 V is also present. Three electrons are added upon this reduction, as has been assessed by comparison of the current intensity with that of an equimolar amount of *N*,*N*′-dimethyl-1[2-diphenylphosphinoferrocenyl] ethylamine added as an internal standard. A rapid chemical reaction follows the reduction ($i_{pa}/i_{pc} = 0.3$ at 2 V s^{-1}),[25] and a new, redox-active compound is formed as indicated by the appearance of two oxidation processes (at +0.26 and +0.65 V). These may be tentatively assigned to the hydride derivative **5** ($E^{\circ\prime}$ in Table 5), which is known to form slowly from **1**$^+$ in the presence of adventitious water.

The isocyanide clusters **18**$^+$ and **19**$^+$ also exhibit two one-electron oxidations. As expected, since three carbonyl ligands have been substituted by better σ-donor and poorer π-acceptor isocyanides, these occur at lower potentials than in cation **1**$^+$. As compiled in Table 5, the redox potentials for the two electron removals occur at very similar potential values (+0.44 and +0.90 V for **18**$^+$). In both cases, only the first oxidation is chemically reversible on the time scale of the cyclic voltammetry, whereas the second oxidation is complicated by a subsequent chemical reaction, which appears faster for **19**$^+$ ($i_{pc}/i_{pa} = 0.4$ at 0.02 V s^{-1}) than for **18**$^+$ ($i_{pc}/i_{pa} = 0.8$ at 0.02 V s^{-1}). In the case of **18**$^+$, a more anodic oxidation process is also observed (at +1.16 V) and is confidently ascribed to the oxidation of the iodine atom[26] of the isocyanide ligands. In the cathodic region, these clusters undergo a multielectron reduction followed by fast chemical reactions. As exemplified in Figure 4, which refers to **2** and **8**, the neutral compounds **2**−**10**, in which one of the three carbonyl groups in cation **1**$^+$ is replaced by a σ-donor anionic ligand, also exhibit two one-electron oxidation processes, cathodically shifted with respect to the oxidations of **1**$^+$. The first oxidation possesses features of chemical reversibility on the time scale of cyclic voltammetry. In contrast, the second oxidation is coupled to chemical complications, the rate of which depends upon the nature of the ligand replacing the carbonyl.

An irreversible, one-electron reduction process is also detected at a very negative potential in the case of the halide derivatives **2**−**4**, which is also followed by chemical complications. For the presence of the positive charge and

(25) Zanello, P. *Inorganic Electrochemistry. Theory, Practice and Application*; RSC: Cambridge, U.K., 2003.
(26) Dryhurst, G.; Elving, P. J. *Anal. Chem.* **1967**, *39*, 606, and references therein.

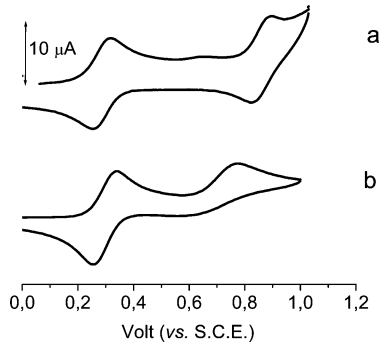

Figure 4. Cyclic voltammograms recorded at a platinum electrode in a CH_2Cl_2 solution of (a) **2** (8.1×10^{-4} M) and (b) **8** (5.6×10^{-4}). $[NBu_4][PF_6]$ (0.2 mol dm^{-3}), supporting electrolyte. Scan rates: 0.2 V s^{-1}.

three strongly π-acidic carbonyl groups, the two oxidations for $\mathbf{1}^+$ are much more positive than those of all other compounds. Indeed, a comparison of the redox potentials of the isocharged $\mathbf{1}^+$, $\mathbf{18}^+$, and $\mathbf{19}^+$ suggests that they are more sensitive to the nature of the terminal ligands, and that Coulombic effects exerted by the decrease of the overall positive charge in **2**−**10** have only a minor effect. A similar behavior has been recently observed in the family of hexanuclear platinum clusters $[\{Pt_6\}(L)_{6-n}(X)_n]^{(2-n)+}$, in which the replacement of one or two apical carbonyl ligands produces significant cathodic shifts of all of the redox changes and causes the appearance of a new oxidation process in the experimental window.[27]

The understanding of the electrochemical behavior of $[\{Pt_3\}L_{3-n}X_n]^{(1-n)+}$ is made easier on the basis of some literature studies on the electronic structure of $[Pt_3(\mu\text{-}L')_3L_3]$ triangular metal clusters,[20a] in which the three terminal ligands, as well as the bridging ones, are identical. As we will see, the electronic structure of these compounds cannot be straightforwardly described using an unsophisticated computational method. In particular, because of their close proximity, the relative order of the relevant frontier orbitals by no way can be accurately reproduced by using any parametrized method. In spite of this, and in absence of a more rigorous theoretical analysis, extended Hückel calculations separately performed by Hoffmann et al.[4a] and by Mealli[4c] are useful to our considerations, provided that one keeps in mind that they certainly give an oversimplified picture of the situation. In the following discussion, we will refer to the results obtained by these authors to propose a qualitative description of the redox behavior, without any attempt to propose new simple theoretical treatments and with the perspective to undertake a more detailed analysis in the future.

With this premise in mind, we get going by dividing the compounds under study into two classes: (i) the cations $\mathbf{1}^+$, $\mathbf{18}^+$, and $\mathbf{19}^+$, with D_{3h} symmetry, and (ii) the neutral clusters **2**−**10**, with C_{2v} symmetry. The electron-precise value for a triangular cluster of metals with a 16-electron configuration is 42, but it has also been shown that, in the presence of π-donor bridging ligands such as PR_2, the orbital arrangement provides counts of 44 electrons.[4a] To simplify the description

(27) Bonaccorsi, C.; Fabrizi de Biani, F.; Leoni, P.; Marchetti, F.; Marchetti, L.; Zanello, P. *Chem. Eur. J.* **2008**, *14*, 847.

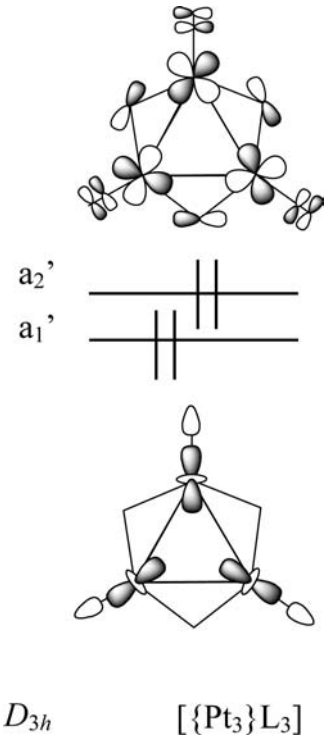

Figure 5. Occupied frontier orbitals for a 44 e^- D_{3h} cluster $[\{Pt_3\}L_3]$.

of the relationship between electronic structures and redox behavior, we will start with the description of the more symmetrical D_{3h} systems. All of the previous studies agree that, with π-donor bridging ligands, there are two easily accessible frontier orbitals very close in energy, so that both the 44 e^- and 42 e^- congeners can possibly be accessed. These frontier orbitals, represented in Figure 5, are a metal−metal bonding combination of $a_{1'}$ symmetry and a metal−metal antibonding combination of $a_{2'}$ symmetry, both lying in the plane of the triangle. In fact, the $a_{2'}$ is stabilized by the bonding combination of metal d orbitals with bridging phosphorus p orbitals. As expected, the relative order of $a_{1'}$ and $a_{2'}$ strongly depends on the size of the Pt_3 triangle; moreover, it also depends on the parameters adopted throughout the calculations. Whatever this order may be, a metal−metal antibonding orbital is filled in the 44 e^- clusters. Thus, the Pt−Pt bond is weakened and the 44 e^- clusters are expected to have long Pt−Pt bonds, or alternatively, they can undergo a distortion from an equilateral to an isosceles triangle by breaking a Pt−Pt bond.[4a−c,20a]

The small gap between $a_{1'}$ and $a_{2'}$ and its fine sensitivity to the computational and geometric parameters prevents the establishment of their real order by a semiempirical method; anyway, a common picture with $a_{2'}$ as the HOMO and $a_{1'}$ as the $HOMO^{-1}$ has generally been proposed. This order would also explain the redox behavior of the D_{3h} clusters $\mathbf{1}^+$, $\mathbf{18}^+$, and $\mathbf{19}^+$. In fact, it is easy to see how the $a_{2'}$ orbital is destabilized as soon as the CO groups are substituted by terminal ligands with a minor π-acceptor ability. This is in agreement with the more accessible oxidation observed for $\mathbf{18}^+$ and $\mathbf{19}^+$.

Let us now examine the C_{2v} neutral clusters **2**−**10**. Also in this case, the first oxidation is easily accessed and is further

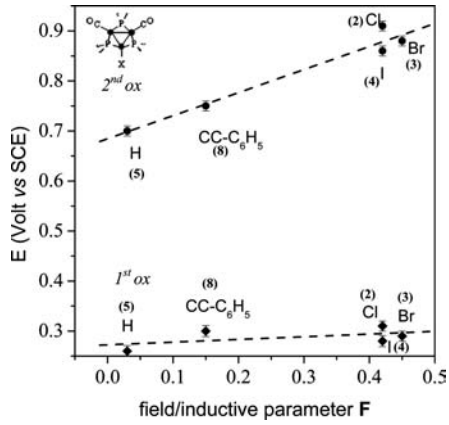

Figure 6. Plot of the $E°$ of the first and second oxidation processes shown by complexes **2**−**5** and **8** vs the Taft parameter F.

cathodically shifted with respect to $\mathbf{18}^+$ and $\mathbf{19}^+$, due to the presence of a strongly σ-donor anionic ligand (and to some charge effects). It is also worth noting that, in the case of the C_{2v} clusters **2**−**10**, the redox potentials of the second oxidation span 280 mV, being therefore much more ligand-affected than the potentials of the first oxidation, which span only 50 mV. Actually, as shown in Figure 6, the redox potentials of the second oxidation show a positive linear relation with the inductive effect of the substituents, as evaluated by the Taft parameter F[28] (best linear fit for the five compounds for which F is known: $E'° = (0.46(6)F + 0.68(2)$ V, with $R = 0.97$ and $P = 0.004$).[29]

On the other hand, it was not possible to obtain any reasonable fit for the redox potentials of the first oxidation (best linear fit: $E'° = (0.05(5)F + 0.27(2))$ V, with $R = 0.53$ and $P = 0.354$).[29] To explain this feature, we propose the molecular orbital scheme shown in Figure 7 in which we compare the orbital energy of $\mathbf{1}^+$ with that of a generic cluster $[\{Pt_3\}(CO)_2X]$. To build this qualitative scheme, we first sketched the relative energy order for the five Pt d orbitals in the fragments $PtCO^+$ (Figure 7a) and PtX (Figure 7e).

Two orbitals ($d_{x^2-y^2}$ and d_{xy}) cannot interact with the terminal ligand and have a similar energy in both $PtCO^+$ and PtX, and the same is almost true for d_{z^2}, destabilized by a σ-antibonding interaction of similar strength. Conversely, d_{xz} and d_{yz} are stabilized by a bonding interaction with the empty CO π^* system in $PtCO^+$, while they are destabilized by an antibonding interaction with the filled p_x and p_y X orbitals in PtX. This difference is mirrored in the orbital ordering of $\mathbf{1}^+$ and $[\{Pt_3\}(CO)_2X]$, obtained upon interaction of the $Pt_2(PR_2)_3(CO)_2$ fragment with $PtCO^+$ and PtX. This would explain the more accessible oxidation observed for **2**−**10**. Moreover, in both cases, only d_{yz} is destabilized (it contributes to the a_2′ orbital), while d_{xz} has a minimal overlap with the orbitals of the $Pt_2(PR_2)_3(CO)_2$ fragment and is expected to remain almost unperturbed. As a result, in $[\{Pt_3\}(CO)_2X]$, the highly localized PtX d_{xz} orbital should be found very close to the HOMO. The redox behavior could

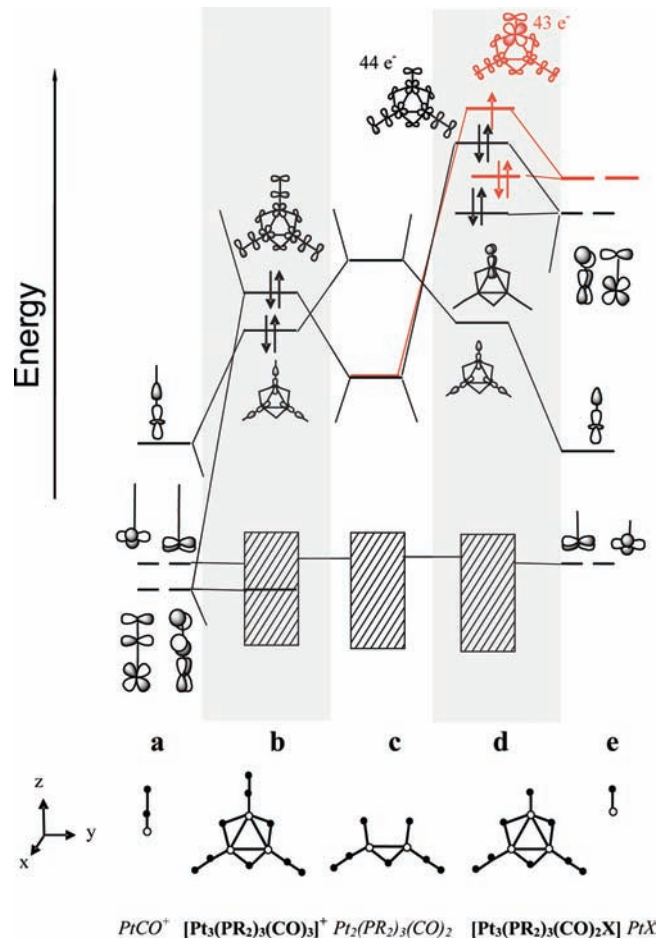

Figure 7. Qualitative picture of the interaction diagram between the fragments $Pt_2(PR_2)_3(CO)_2$ (c) and $PtCO^+$ (a) or PtX (e) to give $[Pt_3(PR_2)_3(CO)_3]^+$ (b) and $[Pt_3(PR_2)_3(CO)_2X]$ (d). Only the higher occupied orbitals are shown.

be explained by assuming that this is the orbital involved in the second electron removal, which for this reason would be more ligand-sensitive; this would require two unpaired electrons for the unstable 42 e$^-$ dications $[\{Pt_3\}(CO)_2X]^{2+}$. Moreover, the second electron should be removed from a nonbonding orbital rather than from an antibonding one. Alternatively, the removal of the first electron from the HOMO would stretch *two* Pt−CO bonds and shrink *one* Pt−X linkage, thus inducing a higher increase of the energy of the PtX d_{yz} orbital (red insert in Figure 7) and imparting a higher contribution from the PtX fragment to the SOMO of the monocation.

Conclusions

We have confirmed here the remarkable robustness of the $Pt_3(\mu\text{-}P^tBu_2)_3$ ($\{Pt_3\}$) core of the 44 e$^-$ derivatives $[\{Pt_3\}(CO)_{3-n}X_n]^{(1-n)+}$, which, thanks to the steric protection offered by the bulky *t*-butyl groups, survives intact under many different reaction conditions. This allowed the achievement, generally in good to excellent yields, of a series of alkynyl derivatives of the general formula $\{Pt_3\}(CO)_2(CC)_n$-R, $\{Pt_3\}(CO)_2$(CC-Ar-X), and $\{Pt_3\}(CO)_2(CC\text{-}Ar)_n$-X. For the presence of different types of aryl groups (phenyl-, thiophene-, or anthracene rings) and of reactive substituents

(28) Hansch, C.; Leo, A.; Taft, R. W. *Chem. Rev.* **199l**, *97*, 165.
(29) P has its usual statistical meaning as "the probability of obtaining the correlation R when the data are uncorrelated". These values of P indicate a probability of 0.4% for the second oxidation fit and 35% for the first oxidation fit.

(R = H, X = CCH, halogen), these are perfectly suited to act as precursors of molecular wires with two {Pt_3} units separated by covalently and strongly bonded alkynyl spacers of different types and length. Functional branched isocyanide derivatives, simply obtained by CO substitution, have also been obtained and have the proper geometric features to behave as precursors of clusters containing planar or nearly planar macrocyclic or dendrimeric structures and of clusters containing porous organometallic solids as well. The new ligands are already, or may easily be transformed into, bifunctional spacers able to connect cluster units. Moreover, they are often conjugated, and this will permit investigation of the cluster-to-cluster electronic communication as mediated by the spacer ligands. The above-described electrochemical characterization of the cluster precursors, which generally show one chemically reversible monoelectronic oxidation, will be of great help in the study of electron transfer processes in extended polycluster structures. On the other hand, the presence of two stable redox states on the cluster synthons may impart interesting redox properties to their multicluster derivatives.

Experimental Section

General Data. All reactions were carried out under a nitrogen atmosphere, by using standard Schlenk techniques. [$Pt_3(\mu$-$P^tBu_2)_3(CO)_3](CF_3SO_3)$ (**1**),[14d] $Pt_3(\mu$-$P^tBu_2)_3(CO)_2Cl$ (**2**),[14a,b] $Pt_3(\mu$-$P^tBu_2)_3(CO)_2H$ (**5**),[17] 1-trimethylsilyl-1,3-butadiyne,[30] 1,4-diethynylbenzene,[31] 2,5-diethynylthiophene,[32] 9,10-diethynylanthracene,[33] CN-C_6H_4-4-I,[34] and CN-C_6H_4-4-CCH[35] were all prepared according to literature procedures or minor modifications thereof. Solvents were dried by conventional methods and distilled under nitrogen prior to use. IR spectra were recorded on a Perkin-Elmer FT-IR spectrometer equipped with a UATR sampling accessory. NMR spectra were recorded on a Varian Gemini 200 BB instrument (200 MHz for ^{1}H) at room temperature (about 293 K) in $CDCl_3$ solutions; frequencies are referenced to the residual resonances of the deuterated solvent (H, ^{13}C), to 85% H_3PO_4 (^{31}P), and to H_2PtCl_6 (^{195}Pt). The symbol # is used to label ^{1}H, ^{13}C, and ^{31}P peaks with ^{195}Pt satellites. Electrochemical measurements were performed in a dichloromethane solution containing [N^nBu_4][PF_6] (0.2 mol dm^{-3}) as a supporting electrolyte. Anhydrous 99.9% dichloromethane was obtained from Aldrich. Electrochemical-grade [N^nBu_4][PF_6] was purchased from Fluka and used as obtained. Cyclic voltammetry was performed in a three-electrode cell containing a platinum working electrode surrounded by a platinum-spiral counter electrode, and an aqueous saturated calomel reference electrode (SCE) mounted with a Luggin capillary. Either a BAS 100A or a BAS 100W electrochemical analyzer were used as a polarizing unit. All the potential values are referred to the SCE. Under the present experimental conditions, the one-electron oxidation of ferrocene occurs at $E^{0\prime} = +0.39$ V. Controlled potential coulometry was performed in an H-shaped cell with anodic and cathodic compartments separated by a sintered-glass disk. The working macroelectrode was a platinum gauze; a mercury pool was used as the counter electrode. Hydrodynamic voltammetry made use of a platinum electrode.

Preparation of $Pt_3(\mu$-$PBut_2)_3(CO)_2Br$ (3). ^{n}Bu_4NBr (290 mg, 0.90 mmol) was added to a green solution of complex **1** (825 mg, 0.66 mmol) in acetone (20 mL). After stirring for 12 h at room temperature, the solvent was removed by an oil pump vacuum, and CH_3CN (10 mL) was added. The microcrystalline brown solid was collected by filtration, washed with CH_3CN, and vaccuum-dried (702 mg, 92%). Anal. calcd for $C_{26}H_{54}BrO_2P_3Pt_3$: C, 27.0; H, 4.71. Found: C, 27.1; H 4.80. ^{1}H NMR:[36] δ 1.44 (vt, $^3J_{HP} + {}^5J_{HP} = 7.4$ Hz, 36 H, CCH_3), 1.38 ppm (d, $^3J_{HP} = 15$ Hz, 18 H, CCH_3). ^{13}C{^{1}H} NMR: δ 172.7# (s, $^1J_{CPt} = 2076$ Hz, CO), 39.8#, 38.6# (m, CCH_3), 33.5, 33.2 ppm (m, CCH_3). IR (CH_2Cl_2): 2027 cm^{-1} ($\nu_{C\equiv O}$).

Preparation of $Pt_3(\mu$-$P^tBu_2)_3(CO)_2I$ (4). Compound **4** was prepared using a procedure identical to that used for **3** by reacting **1** (300 mg, 0,24 mmol) with ^{n}Bu_4NI (110 mg, 0,30 mmol). Yield: 94% (brown solid, 272 mg). Anal. calcd for $C_{26}H_{54}IO_2P_3Pt_3$: C, 25.9; H, 4.52. Found: C, 26.1; H, 4.43. ^{1}H NMR:[36] δ 1.44 (vt, $^3J_{HP} + {}^5J_{HP} = 7.5$ Hz, 36 H, CCH_3), 1.38 ppm (d, $^3J_{HP} = 15$ Hz, 18 H, CCH_3). ^{13}C{^{1}H} NMR: δ 173.3# (s, $^1J_{CPt} = 2096$ Hz, CO), 39.9#, 38.7# (m, CCH_3), 34.3, 33.4 ppm (m, CCH_3). IR (CH_2Cl_2): 2024 cm^{-1} ($\nu_{C\equiv O}$).

Preparation of $Pt_3(\mu$-$P^tBu_2)_3(CO)_2CC$-$SiMe_3$ (6). To a stirred solution of **2** (120 mg, 0.108 mmol) in diethylamine (25 mL) were added trimethylsilylacetylene (17 μL, 0.120 mmol) and CuI (0.21 mg, 1.10×10^{-3} mmol). The brown solution was stirred at room temperature for 20 h, after which all volatile components were removed under reduced pressure. The residue was dissolved in Et_2O and passed through a silica gel column and eluted with *n*-hexane/CH_2Cl_2 (8: 1, v/v). Removal of the solvents in vacuo gave the title complex as a reddish-brown solid in 88% yield (112 mg). Anal. calcd for $C_{31}H_{63}O_2P_3Pt_3Si$: C, 31.7; H, 5.41. Found: C, 31.6; H, 5.60. ^{1}H NMR:[36] δ 1.38 (vt, $^3J_{HP} + {}^5J_{HP} = 7.3$ Hz, 36 H, CCH_3), 1.31 (d, $^3J_{HP} = 14$ Hz, 18 H, CCH_3), 0.14 ppm (s, 9 H, $SiCH_3$). ^{13}C{^{1}H} NMR: δ 175.2# (s, $^1J_{CPt} = 2019$ Hz, $^2J_{CPt} = 130$, 39 Hz, CO), 126.2# (s, $^2J_{CPt} = 406$ Hz, Pt−C≡CSi), 103.7# (s, $^1J_{CPt} = 1544$ Hz, Pt−*C*≡CSi), 39.0#, 38.7# (m, *C*CH_3), 33.5 (br s, C*C*H_3), 1.32 ppm (s, $SiCH_3$). IR (solid state): 2022 ($\nu_{C\equiv O}$), 1978 ($\nu_{C\equiv C}$) cm^{-1}.

Complex **6**was also prepared with a different procedure: **2** (50 mg, 0.045 mmol) was dissolved in THF (5 mL) and cooled to −60 °C. $LiCCSiMe_3$ (0.5 M in THF, 90 μL, 0.045 mmol) was added, and the reaction mixture was stirred for 1 h before being brought to room temperature. After filtration and evaporation of the solvent, **6** was obtained as a brown solid in 60% yield.

$Pt_3(\mu$-$P^tBu_2)_3(CO)_2CC$-CC-$SiMe_3$ (7). Complex **2** (146 mg, 0.131 mmol) and a THF solution containing 0.195 mmol of 1-trimethylsilylbutadiyne were combined in a procedure analogous to that for **6**. An identical workup gave **7** as a brown solid (132 mg, 84%). Anal. calcd for $C_{33}H_{63}O_2P_3Pt_3Si$: C, 33.1; H 5.30. Found: C, 33.2; H, 5.45. ^{1}H NMR:[36] δ 1.37 (vt, $^3J_{HP} + {}^5J_{HP} = 7.5$ Hz, 36 H, CCH_3), 1.32 (d, $^3J_{HP} = 15.5$ Hz, 18 H, CCH_3), 0.19 ppm (s, 9 H, $SiCH_3$). ^{13}C{^{1}H} NMR: δ 174.6# (s, $^1J_{CPt} = 2024$ Hz, $^2J_{CPt} = 131$, 43 Hz, CO), 104.5# (s, $^2J_{CPt} = 517$ Hz, Pt−C≡C), 93.0# (s, $^3J_{CPt} = 64$ Hz, C≡CSi), 85.2# (s, $^1J_{CPt} = 1764$ Hz, Pt−C≡C), 79.1 (s, C≡CSi), 38.8# (m, CCH_3), 35.5 (br s, CCH_3), 0.6 ppm (s, $SiCH_3$). IR (solid state): 2112, ($\nu_{C\equiv C}$), 2020 ($\nu_{C\equiv O}$) cm^{-1}.

(30) Bruce, M. I.; Low, P. J.; Werth, A.; Skelton, B. W.; White, A. H. *J. Chem. Soc., Dalton Trans.* **1996**, 1551.
(31) Plater, M. J.; Sinclair, J. P.; Aiken, S.; Gelbrich, T.; Hursthouse, M. B. *Tetrahedron* **2004**, *60*, 6385.
(32) Neenan, T. X.; Whitesides, G. M. *J. Org. Chem.* **1988**, *53*, 2489.
(33) Khan, M. S.; Al-Mandhary, M. R. A.; Al-Suti, M. K.; Al-Battashi, F. R.; Al-Saadi, S.; Ahrens, B.; Bjernemose, J. K.; Mahon, M. F.; Raithby, P. R.; Younus, M.; Chawdhury, N.; Köhler, A.; Marseglia, E. A.; Tedesco, E.; Feeder, N.; Teat, S. J. *Dalton Trans.* **2004**, 2377.
(34) Weber, W. P.; Gokel, G. W. *Tetrahedron Lett.* **1972**, *17*, 1637.
(35) Jia, G.; Payne, N. C.; Vittal, J. J.; Puddephatt, R. J. *Organometallics* **1993**, *12*, 4771.

(36) For ^{31}P and ^{195}Pt NMR data, see Table 1.

$Pt_3(\mu\text{-}P^tBu_2)_3(CO)_2CC\text{-}C_6H_5$ (8). Compound **8** was prepared from **2** (130 mg, 0.117 mmol) and phenylacetylene (15 μL, 0.137 mmol) in accordance with the general procedure. Purification by column chromatography (silica gel, *n*-hexane) gave **8** (124 mg, 90%) as a greenish-brown solid. Anal. calcd for $C_{34}H_{59}O_2P_3Pt_3$: C, 34.7; H, 5.05. Found: C, 34.6; H, 4.94. ^{1}H NMR:[36] δ 7.41 (d, $^3J_{HH}$ = 7 Hz, 2 H, C_6H_5), 7.29 (t, $^3J_{HH}$ = 7 Hz, 2 H, C_6H_5), 7.16 (t, $^3J_{HH}$ = 7 Hz, 1 H, C_6H_5), 1.47 (vt, $^3J_{HP} + {}^5J_{HP}$ = 7.5 Hz, 36 H, CCH_3), 1.39 ppm (d, $^3J_{HP}$ = 15.6 Hz, 18 H, CCH_3). ^{13}C{^{1}H} NMR: δ 175.5# (s, $^1J_{CPt}$ = 2029 Hz, $^2J_{CPt}$ = 130, 42 Hz, CO), 130.8# (s, C_6H_5), 130.0# (s, $^3J_{CPt}$ = 39 Hz, C_6H_5), 128.2 (s, C_6H_5), 124.2 (s, C_6H_5), 121.7#(s, $^2J_{CPt}$ = 478 Hz, Pt−C≡*C*), 87.4# (s, $^1J_{CPt}$ = 1696 Hz, Pt−*C*≡C), 39.0# (m, *C*CH_3), 33.5 ppm (br s, C*C*H_3). IR (solid state): 2108 ($\nu_{C\equiv C}$), 2026 ($\nu_{C\equiv O}$) cm^{-1}.

$Pt_3(\mu\text{-}P^tBu_2)_3(CO)_2CC\text{-}C_6H_4\text{-}Br$ (9). Compound **9** was prepared from **2** (150 mg, 0.135 mmol) and 1-bromo-4-ethynylbenzene (30 mg, 0.166 mmol) in accordance with the general procedure. Purification by column chromatography (silica gel, 1:5 CH_2Cl_2/*n*-hexane) gave **9** (154 mg, 91%) as a greenish-brown solid. Anal. calcd for $C_{34}H_{58}BrO_2P_3Pt_3$: C, 32.5; H, 4.65. Found: C, 32.7; H, 4.59. ^{1}H NMR:[36] δ 7.36 (d, $^3J_{HH}$ = 8.4 Hz, 2 H, C_6H_4), 7.24 (t, $^3J_{HH}$ = 8.4 Hz, 2 H, C_6H_4), 1.41 (vt, $^3J_{HP} + {}^5J_{HP}$ = 7.6 Hz, 36 H, CCH_3), 1.33 ppm (d, $^3J_{HP}$ = 15.4 Hz, 18 H, CCH_3). ^{13}C{^{1}H} NMR: δ 175.0# (s, $^1J_{CPt}$ = 2020 Hz, $^2J_{CPt}$ = 129, 41 Hz, CO), 132.2 (s, C_6H_4), 128.5# (s, $^3J_{CPt}$ = 38, C_6H_4), 120.3# (s, $^2J_{CPt}$ = 476 Hz, Pt−C≡C), 118.1 (s, C_6H_4), 89.1# (s, $^1J_{CPt}$ = 1690 Hz, Pt−C≡C), 38.8# (m, CCH_3), 33.4 ppm (br s, CCH_3). IR (CH_2Cl_2): 2103 ($\nu_{C\equiv C}$), 2023 ($\nu_{C\equiv O}$) cm^{-1}.

$Pt_3(\mu\text{-}P^tBu_2)_3(CO)_2CC\text{-}C_6H_4\text{-}CCH$ (10). Compound **10** was synthesized from **2** (100 mg, 0.090 mmol) and freshly prepared 1,4-diethynylbenzene (15 mg, 0.119 mmol) in accordance with the general procedure. A similar workup gave a greenish-brown solid (106 mg, 88%). Anal. calcd for $C_{36}H_{59}O_2P_3Pt_3$: C, 36.0; H, 4.95. Found: C, 35.8; H, 4.74. ^{1}H NMR:[36] δ 7.39 (d, $^3J_{HH}$ = 8.2 Hz, 2 H, C_6H_4), 7.32 (2, $^3J_{HH}$ = 8.2 Hz, 2 H, C_6H_4), 3.11 (s, 1 H, CCH), 1.41 (vt, $^3J_{HP} + {}^5J_{HP}$ = 7.6 Hz, 36 H, CCH_3), 1.34 ppm (d, $^3J_{HP}$ = 15.5 Hz, 18 H, CCH_3). ^{13}C{^{1}H} NMR: δ 175.0# (s, $^1J_{CPt}$ = 2019 Hz, $^2J_{CPt}$ = 130, 45 Hz, CO), 131.7 (s, C_6H_4), 130.5 (s, C_6H_4), 121.5# (s, $^2J_{CPt}$ = 488 Hz, Pt−C≡*C*), 117.6 (s, C_6H_4), 91.3# (s, $^1J_{CPt}$ = 1715 Hz, Pt−*C*≡C), 84.5 (s, *C*≡CH), 77.0 (s, C≡*C*H), 38.9#, 38.7# (m, *C*CH_3), 33.4 ppm (br s, C*C*H_3). IR (solid state): 3275 ($\nu_{C\equiv CH}$), 2099 ($\nu_{C\equiv C}$), 2014 ($\nu_{C\equiv O}$) cm^{-1}.

$Pt_3(\mu\text{-}P^tBu_2)_3(CO)_2CC\text{-}C_4H_2S\text{-}CCH$ (11). Compound **11** was prepared from **2** (122 mg, 0.110 mmol) and freshly prepared 2,5-diethynylthiophene (20 mg, 0.151 mmol) in accordance with the general procedure. A similar workup gave a greenish-brown solid (116 mg, 86%). Anal. calcd for $C_{34}H_{57}O_2P_3Pt_3S$: C, 33.8; H, 4.76. Found: C, 33.7; H, 4.87. ^{1}H NMR (C_6D_6):[36] δ 7.01 (d, $^3J_{HH}$ = 3.7 Hz, 1 H, C_4H_2S), 6.82 (d, $^3J_{HH}$ = 3.7 Hz, 1 H, C_4H_2S), 2.87 (s, 1 H, CCH), 1.43 (vt, $^3J_{HP} + {}^5J_{HP}$ = 7.7 Hz, 36 H, CCH_3), 1.16 ppm (d, $^3J_{HP}$ = 15.4 Hz, 18 H, CCH_3). ^{13}C{^{1}H} NMR (C_6D_6): δ 175.7# (s, $^1J_{CPt}$ = 2028 Hz, $^2J_{CPt}$ = 128, 39 Hz, CO), 133.3, 128.3, 127.1, 119.2 (s, C_4H_2S), 115.0# (s, $^2J_{CPt}$ = 526 Hz, Pt−C≡C), 95.6# (s, $^1J_{CPt}$ = 1602 Hz, Pt−C≡C), 80.8 (s, C≡CH), 78.1 (s, C≡CH), 39.0# (m, CCH_3), 33.6 ppm (br s, CCH_3). IR (solid state): 3276 ($\nu_{\equiv CH}$), 2099, 2082 ($\nu_{C\equiv C}$), 2017 ($\nu_{C\equiv O}$) cm^{-1}.

$Pt_3(\mu\text{-}P^tBu_2)_3(CO)_2CC\text{-}9\text{-}C_{14}H_8\text{-}10\text{-}CCH$ (12). Compound **12** was prepared from **2** (145 mg, 0.130 mmol) and freshly prepared 9,10-diethynylanthracene (42 mg, 0.186 mmol) in accordance with the general procedure. A similar workup gave a reddish solid (129 mg, 76%). Anal. calcd for $C_{44}H_{63}O_2P_3Pt_3$: C, 40.6; H, 4.88. Found: C, 40.7; H, 4.69. ^{1}H NMR:[36] δ 8.31 (m, 4 H, $C_{14}H_8$), 7.32 (m, 4 H, $C_{14}H_8$), 3.81 (s, 1 H, C≡CH), 1.42 (vt, $^3J_{HP} + {}^5J_{HP}$ = 8.0 Hz, 36 H, CCH_3), 1.34 ppm (d, $^3J_{HP}$ = 15.2 Hz, 18 H, CCH_3). ^{13}C{^{1}H} NMR: δ 174.7# (s, $^1J_{CPt}$ = 2000 Hz, CO), 133.2, 129.4, 129.0, 127.4, 126.9, 126.4, 125.3, 124.5 (s, arom.), 89.8 (s, C≡*C*H), 87.2 (s, *C*≡CH), 38.9# (m, *C*CH_3), 33.5 ppm (br s, C*C*H_3). IR (CH_2Cl_2): 3300 ($\nu_{\equiv CH}$), 2080 ($\nu_{C\equiv C}$), 2022 ($\nu_{C\equiv O}$) cm^{-1}.

Preparation of $Pt_3(\mu\text{-}P^tBu_2)_3(CO)_2CCH$ (13). Method a. A solution of **2** (111 mg, 0.10 mmol) and CuI (0.19 mg, 1.00×10^{-3} mmol) in $NHEt_2$ (20 mL) was cooled to 0 °C under a dinitrogen atmosphere. The flask was evacuated and filled with acetylene (1 atm). The solution was stirred for 5 h at 0 °C and then for 3 h at room temperature. A workup according to the general procedure gave **13** as a brown solid (88 mg, 80%).

Method b. Desilylation of $Pt_3(\mu\text{-}P^tBu_2)_3(CO)_2CCSiMe_3$ (**6**): TBAF (1 M solution in THF, 115 μL, 0.155 mmol) was added to a solution of **6** (135 mg, 0.155 mmol) in THF (15 mL). After stirring for 3 h, all volatiles were removed in vacuo, and the residue was extracted with *n*-hexane to give, after chromatography (silica gel, eluent: 1:8 CH_2Cl_2/*n*-hexane), 89 mg of 13 (70%). Anal. calcd for $C_{28}H_{55}O_2P_3Pt_3$: C, 30.5; H, 5.03. Found: C, 30.4; H, 4.91. ^{1}H NMR (C_6D_6):[36] δ 3.37# (s, $^3J_{HPt}$ = 71 Hz, 1 H, CCH), 1.45 (vt, $^3J_{HP} + {}^5J_{HP}$ = 7.6 Hz, 36 H, CCH_3), 1.18 ppm (d, $^3J_{HP}$ = 15 Hz, 18 H, CCH_3). ^{13}C{^{1}H} NMR (C6D6): δ 175.0# (s, $^1J_{CPt}$ = 2044 Hz, $^2J_{CPt}$ = 132, 41 Hz, CO), 107.1# (s, $^2J_{CPt}$ = 477 Hz, Pt−C≡CH), 76.0# (s, $^1J_{CPt}$ = 1668 Hz, Pt−C≡CH), 38.8# (m, CCH_3), 35.5 ppm (br s, CCH_3). IR (solid state): 3292 ($\nu_{\equiv CH}$), 1970 ($\nu_{C\equiv C}$), 2009 ($\nu_{C\equiv O}$) cm^{-1}.

Preparation of $Pt_3(\mu\text{-}P^tBu_2)_3(CO)_2CC\text{-}CCH$ (14). Method a. Compound **14** was prepared starting from **2** (90 mg; 0.081 mmol) and HCC-CCH[37] (0.150 mmol as a 2.5 M solution in THF) in accordance with the general procedure. A similar workup gave a brown powder of **14** (73 mg, 80%).

Method b. Desilylation of $Pt_3(\mu\text{-}PBu^t_2)_3(CO)_2CC\text{-}CC\text{-}SiMe_3$ (**7**): (i, with TBAF) 122 μL of a 1 M THF solution of TBAF (0.122 mmol) was added to a THF solution (10 mL) of **7** (144 mg, 0.120 mmol). After stirring for 4 h, all volatiles were removed in vacuo. The residue was extracted with *n*-hexane and filtered over a silica pad. Evaporation to dryness yielded **14** as a brown powder (105 mg, 78%). (ii, with K_2CO_3) K_2CO_3 (45 mg, 0.326 mmol) and **7** (162 mg, 0.135 mmol) were dissolved in 8 mL of a MeOH/THF mixture (v/v = 1:1). The reaction mixture was stirred at room temperature for 16 h, and the volatiles were removed in vacuo. The residue was extracted with *n*-hexane, and the solvent was removed in vacuo, yielding **14** (140 mg, 92%). (iii, with KF) A MeOH (3 mL) solution containing KF (5 mg, 0.086 mmol) was added to a solution of complex **7** (86 mg, 0.072 mmol) in THF (6 mL). The resulting mixture was stirred for 12 h at room temperature, and the solvent was removed under reduced pressure. The solid residue was extracted with *n*-hexane and filtered over a silica pad. Removal of the solvent to dryness yielded 60 mg of **14** (74%). (iv, with NaOH) To a THF solution (5 mL) of **7** (74 mg, 0.062 mmol) were added 3 mL of MeOH and 65 μL of a 1 M NaOH aqueous solution (0.065 mmol). After stirring at room temperature for 1 h, 5 mL of THF was additionally added in the above reaction mixture; then, it was washed with H_2O until the pH approximately equaled 7. The THF solution was dried over anhydrous $MgSO_4$. Evaporation of the solvent gave **14** (58 mg, 83%). Anal. calcd for $C_{30}H_{55}O_2P_3Pt_3$: C, 32.0; H, 4.92. Found: C, 32.1; H 4.80. ^{1}H NMR:[36] δ 2.13# (s, $^5J_{HPt}$ = 13 Hz, 1 H, CCH), 1.39 (vt, $^3J_{HP} + {}^5J_{HP}$ = 7.4 Hz, 36 H, CCH_3), 1.33 ppm (d, $^3J_{HP}$ = 15 Hz, 18 H, CCH_3). ^{13}C{^{1}H} NMR: δ 174.5# (s, $^1J_{CPt}$ = 2023 Hz, $^2J_{CPt}$ = 130, 46 Hz, CO), 102.8# (s,

(37) Butadiyne was prepared from the commercially available 1,4-bis(trimethylsilyl)-1,3-butadiyne by desilylation reaction and handled in THF solution at −34 °C.

Table 6. Crystal Data and Structure Refinements

compound	**2**·acetone	**8**	**9**
empirical formula	$C_{29}H_{60}ClO_3P_3Pt_3$	$C_{34}H_{59}O_2P_3Pt_3$	$C_{34}H_{58}BrO_2P_3Pt_3$
fw	1170.40	1177.99	1256.89
cryst syst	monoclinic	monoclinic	orthorhombic
space group	$P2_1/m$ (No. 11)	$P2_1/n$ (No. 14)	$Cmcm$ (No. 63)
a/Å	9.151(2)	12.078(2)	15.983(2)
b/Å	17.709(2)	15.531(2)	19.038(2)
c/Å	12.006(2)	21.956(2)	13.937(2)
β/deg	91.09(1)	95.21(1)	
U/Å^3	1945.3(5)	4101.6(9)	4240.7(8)
Z	2	4	4
D_{calcd}/Mg·m^{-3}	1.998	1.919	1.969
μ/mm^{-1}	10.978	10.412	10.950
no. measured	4094	10373	2766
no. unique [R_{int}]	3139 [0.0655]	8442 [0.0511]	2245 [0.0571]
no. parameters	169	379	122
R_1, wR_2 [$I > 2\sigma(I)$][a]	0.0696, 0.1581	0.0483, 0.1033	0.0398, 0.0797
R_1, wR_2 [all data][a]	0.1170, 0.1842	0.0869, 0.1198	0.0680, 0.0898
goodness of fit[a] on F^2	1.030	1.006	1.018

[a] $R(F_o) = \sum||F_o| - |F_c||/\sum|F_o|$; $Rw(F_o^2) = [\sum[w(F_o^2-F_c^2)^2]/\sum[w(F_o^2)^2]]^{1/2}$; $w = 1/[\sigma^2(F_o^2) + (AQ)^2 + BQ]$ where $Q = [MAX(F_o^2,0) + 2F_c^2]/3$; GOF = $[\sum[w(F_o^2 - F_c^2)^2]/(N - P)]^{1/2}$, where N and P are the numbers of observations and parameters, respectively.

$^2J_{CPt}$ = 506 Hz, Pt−C≡*C*), 82.6# (s, $^1J_{CPt}$ = 1748 Hz, Pt−*C*≡C), 72.9 (s, $^3J_{CPt}$ = 58 Hz, *C*≡CH), 62.2 (s, C≡*C*H), 39.0# (m, *C*CH$_3$), 33.4 ppm (br s, C*C*H$_3$). IR (solid state): 3299 ($\nu_{\equiv CH}$), 2121 ($\nu_{C\equiv C}$), 2015 ($\nu_{C\equiv O}$) cm^{-1}.

Preparation of Pt$_3$(μ-P^{t}Bu$_2$)$_3$(CO)$_2$(CC-C$_6$H$_4$)$_2$-I (15). To a solution of **10** (130 mg, 0.108 mmol) and 1,4-diiodobenzene (66 mg, 0.200 mmol) in NHEt$_2$ (20 mL) were added CuI (0.21 mg, 1.10×10^{-3} mmol) and Pd(PPh$_3$)$_2$Cl$_2$ (0.77 mg, 1.10×10^{-3} mmol). The brown solution was stirred at room temperature for 24 h, and the solvent was removed under reduced pressure. The residue was extracted with *n*-hexane to give, after chromatography (silica gel, eluent: *n*-hexane), **15** as a greenish-brown solid (97 mg, 65%). Anal. calcd for $C_{42}H_{62}IO_2P_3Pt_3$: C, 35.9; H, 4.45. Found: C, 35.8; H, 4.60. ^{1}H NMR:[36] δ 7.68 (d, $^3J_{HH}$ = 7.4 Hz, 2 H, C$_6$H$_4$I), 7.41 (d, $^3J_{HH}$ = 8.2 Hz, 2 H, C$_6$H$_4$), 7.35 (d, $^3J_{HH}$ = 8.2 Hz, 2 H, C$_6$H$_4$), 7.25 (d, $^3J_{HH}$ = 7.4 Hz, 2 H, C$_6$H$_4$I), 1.42 (vt, $^3J_{HP}$ + $^5J_{HP}$ = 7.4 Hz, 36 H, CCH$_3$), 1.34 ppm (d, $^3J_{HP}$ = 15.7 Hz, 18 H, CCH$_3$). ^{13}C{^{1}H} NMR: δ 175.0# (s, $^1J_{CPt}$ = 2023 Hz, $^2J_{CPt}$ = 128, 46 Hz, CO), 137.1, 132.9, 131.2, 130.7, 130.1, 123.2 (s, C$_6$H$_4$), 121.6# (s, $^2J_{CPt}$ = 498 Hz, Pt−C≡C), 118.4 (s, C$_6$H$_4$), 93.6 (s, C$_6$H$_4$I), 91.8 (s, C≡C), 88.6 (s, C≡C), 38.9# (m, CCH$_3$), 33.5 ppm (br s, CCH$_3$). IR (solid state): 2101 ($\nu_{C\equiv C}$), 2017 ($\nu_{C\equiv O}$) cm^{-1}.

Preparation of Pt$_3$(μ-P^{t}Bu$_2$)$_3$(CO)$_2$(CC-C$_6$H$_4$)$_3$-CCH (16). Compound **16** was prepared by using a procedure identical to that used for **15**, starting from **15** (90 mg, 0.065 mmol) and 1,4-diethynylbenzene (15 mg, 0.119 mmol). A similar workup gave **16** as a greenish-brown solid in 62% yield (55 mg). Anal. calcd for $C_{52}H_{67}O_2P_3Pt_3$: C, 44.5; H, 4.82. Found: C, 44.7; H, 4.90. ^{1}H NMR:[36] δ 7.54−7.49 (m, 12 H, C$_6$H$_4$), 3.26 (s, 1 H, CCH), 1.42 (vt, $^3J_{HP}$ + $^5J_{HP}$ = 8.0 Hz, 36 H, CCH$_3$), 1.34 ppm (d, $^3J_{HP}$ = 16.0 Hz, 18 H, CCH$_3$). IR (solid state): 3276 ($\nu_{\equiv CH}$), 2100 ($\nu_{C\equiv C}$), 2017 ($\nu_{C\equiv O}$) cm^{-1}.

Preparation of Pt$_3$(μ-P^{t}Bu$_2$)$_3$(CNC$_6$H$_4$-p-I)$_2$H (17). CNC$_6$H$_4$-*p*-I (50.4 mg, 0.220 mmol) was added to an orange solution of complex **5** (110 mg, 0.102 mmol) in toluene (5 mL). After 2 h, the solvent was evaporated. The residue was suspended in acetonitrile, and the orange solid which precipitated out was separated by filtration and vaccuum-dried (113 mg, 75% yield). Anal. calcd for $C_{52}H_{67}O_2P_3Pt_3$: C, 39.8; H, 4.29; N, 1.9. Found: C, 39.7; H, 4.50; N, 1.9. ^{1}H NMR (C$_6$D$_6$):[36] δ 7.12 (d, $^3J_{HH}$ = 8.5 Hz, 4 H, C$_6$H$_4$), 6.64 (d, $^3J_{HH}$ = 8.5 Hz, 4 H, C$_6$H$_4$), 1.52 (vt, $^3J_{HP}$ + $^5J_{HP}$ = 7.1 Hz, 36 H, CCH$_3$), 1.46 (d, $^3J_{HP}$ = 13.7 Hz, 18 H, CCH$_3$), −5.71# ppm (dt, $^3J_{HP}$ = 13.4 Hz, $^2J_{HP}$ = 9.0 Hz, $^1J_{HPt}$ = 1285 Hz, 1 H, Pt−H).^{13}C{^{1}H} NMR (C$_6$D$_6$): δ 139.2 (s, C$_6$H$_4$), 125.9 (s, C$_6$H$_4$), 38.1#, 36.8# (m, *C*CH$_3$), 33.9 ppm (br. s, C*C*H$_3$). IR (solid state): 2067, 2022 cm^{-1} ($\nu_{C\equiv N}$).

Preparation of [Pt$_3$(μ-P^{t}Bu$_2$)$_3$(CNC$_6$H$_4$-p-I)$_3$]OTf (18). CNC$_6$H$_4$-*p*-I (130 mg, 0.57 mmol) was added to an acetone solution (5 mL) of complex **1** (125 mg, 0.10 mmol). After 30 min of stirring at room temperature, the green solution was concentrated to 1 mL, and Et$_2$O was added. The green solid which precipitates out was filtered and vaccuum-dried (171 mg, 92%). Anal. calcd for $C_{46}H_{66}F_3I_3N_3O_3P_3Pt_3S$: C, 29.8; H, 3.58. Found: C, 29.7; H, 3.80. ^{1}H NMR:[36] δ 7.90 (d, $^3J_{HH}$ = 8.2 Hz, 6 H, C$_6$H$_4$), 7.20 (d, $^3J_{HH}$ = 8.2 Hz, 6 H, C$_6$H$_4$), 1.39 ppm (vt, $^3J_{HP}$ + $^5J_{HP}$ = 7.4 Hz, 54 H, CCH$_3$). ^{13}C{^{1}H} NMR: δ 139.5 (s, C$_6$H$_4$), 135.0# (s, $^1J_{CPt}$ = 2061 Hz, $^2J_{CPt}$ = 84 Hz, CN), 127.4 (s, C$_6$H$_4$), 126.4 (s, C$_6$H$_4$), 95.6 (s, C$_6$H$_4$), 38.8# (m, CCH$_3$), 33.3 ppm (s, CCH$_3$). IR (CH$_2$Cl$_2$): 2133 cm^{-1} ($\nu_{C\equiv N}$).

Preparation of Pt$_3$(μ-P^{t}Bu$_2$)$_3$(CNC$_6$H$_4$-p-CCH)$_3$OTf (19). Compound **19** was prepared using a procedure identical to that used for **18** starting from **1** and CNC$_6$H$_4$-*p*-CCH (green powder, 94% yield). Anal. calcd for $C_{52}H_{69}F_3N_3O_3P_3Pt_3S$: C, 40.3; H, 4.48. Found: C, 40.4; H, 4.29. ^{1}H NMR:[36] δ 7.65 (d, $^3J_{HH}$ = 8.3 Hz, 6 H, C$_6$H$_4$), 7.46 (d, $^3J_{HH}$ = 8.3 Hz, 6 H, C$_6$H$_4$), 3.32 (s, 1 H, CCH), 1.40 ppm (vt, $^3J_{HP}$ + $^5J_{HP}$ = 7.5 Hz, 54 H, CCH$_3$). ^{13}C{^{1}H} NMR: δ 134.9# (s, $^1J_{CPt}$ = 2058 Hz, $^2J_{CPt}$ = 79 Hz, CN), 133.9 (s, C$_6$H$_4$), 127.6 (s, C$_6$H$_4$), 125.0 (s, C$_6$H$_4$), 124.2 (s, C$_6$H$_4$), 81.8 (s, C≡CH), 81.0 (s, C≡CH), 38.9# (m, CCH$_3$), 33.3 ppm (s, CCH$_3$). IR (CH$_2$Cl$_2$): 3300 ($\nu_{\equiv CH}$), 2135 ($\nu_{C\equiv N}$), 2064 cm^{-1} ($\nu_{C\equiv C}$).

X-Ray Crystallography. The X-ray diffraction experiments were carried out at room temperature (T = 293 K) by means of a Bruker P4 diffractometer operating with graphite-monochromated Mo Kα radiation. The sample of **2**·0.5acetone was sealed in a glass capillary under a dinitrogen atmosphere; those of **8** and **9** were glued at the end of glass fibers. The intensity data collection was carried out using the $\omega/2\theta$ scan mode, collecting a redundant set of data.

Three standard reflections were measured every 97 measurements to check sample decay. The intensities were corrected for Lorentz and polarization effects and for absorption by means of a Gaussian method based on the crystal shape.[38] The structure solutions were obtained by means of the automatic direct methods contained in SHELXS97[39] for compounds **2**·0.5acetone and **8** and in SIR-92[40] for compound **9**. The refinements, based on full-matrix least-squares on F^2, were done by means of the SHELXL97[39] program. Some other utilities contained in the WINGX suite[41] were also used. The more relevant crystal parameters for the three compounds are listed in Table 6.

The structure solution of **2**·acetone was found in the centrosymmetric space group $P2_1/m$. The asymmetric unit consists of one half of a cluster molecule and one half molecule of a lattice solvent, both doubled by the mirror plane at y = 1/4 (Wickoff position *e*). Disorder is present both in the phosphido methyl groups and in the lattice solvent. As regards the former, the refinement was performed with unconstrained anisotropic thermal parameters for carbon atoms and the hydrogen atoms statistically distributed in two positions, corresponding to a 60° rotation of the methyl group. Concerning the latter, the atomic coordinates of an acetone molecule, coming from a well-refined structure present in the literature, were introduced in the model

(38) Spek, A. L. *Acta Crystallogr., Sect. A* **1990**, *46*, C34.
(39) Sheldrick, G. M. *SHELX97*, release 97-2; Institüt für Anorganische Chemie der Universität: Göttingen, Germany, 1998.
(40) Altomare, A.; Cascarano, G.; Giacovazzo, C.; Guagliardi, A. *J. Appl. Crystallogr.* **1993**, *26*, 343.

Chart 1. Structures of Complexes **2**−**19** (*t*-butyls omitted for clarity)

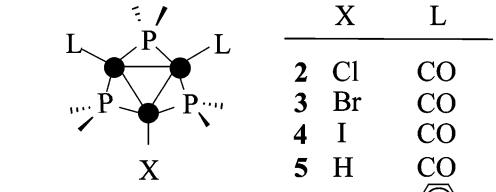

	X	L
2	Cl	CO
3	Br	CO
4	I	CO
5	H	CO
17	H	CN–C$_6$H$_4$–I

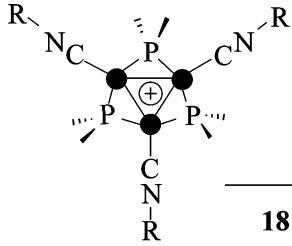

	R
18	–C$_6$H$_4$–I
19	–C$_6$H$_4$–C≡CH

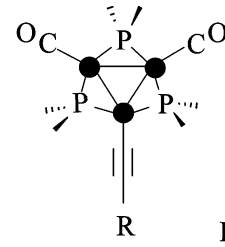

	R
6	–SiMe$_3$
7	–C≡C–SiMe$_3$
8	–C$_6$H$_5$
9	–C$_6$H$_4$–Br
10	–C$_6$H$_4$–C≡CH
11	–C$_4$H$_2$S–C≡CH
12	–C$_{14}$H$_8$–C≡CH
13	–H
14	–C≡CH
15	–C$_6$H$_4$–C≡C–C$_6$H$_4$–I
16	–C$_6$H$_4$–C≡C–C$_6$H$_4$–C≡C–C$_6$H$_4$–C≡CH

and allowed to move as a rigid group with isotropic thermal parameters. The final refinement cycle gave the reliability factors listed in Table 6.

The asymmetric unit in the structure of compound **8** is made up of one molecule. The structure was refined using full-matrix least-squares methods using anisotropic thermal parameters for all non-hydrogen atoms. The shape of thermal ellipsoids of some methyl groups suggested that some amount of orientation disorder may be present in the crystal. Actually, it was more reduced than that found in the crystal of **2**·acetone, and we consented that the thermal factors incorporate the possible disorder. The last refinement cycle gave the reliability factors listed in Table 6.

The asymmetric unit in the structure of compound **9** is made by one-fourth of a molecule placed on the Wickoff position *c*, site symmetry *m*2*m*. The refinement was done using full-matrix least-squares methods using anisotropic thermal parameters for all non-hydrogen atoms. The final reliability factors are listed in Table 6.

Acknowledgment. This work was supported by the Ministero dell'Istruzione, dell'Università e della Ricerca (MIUR), Programmi di Rilevante Interesse Nazionale, PRIN 2006−2007, and by the University of Pisa (Progetti di Ricerca 2006—Scienze e tecnologie dei nano/microsistemi). The authors acknowledge Dr. Carlo Mealli for the helpful discussion.

Supporting Information Available: X-ray crystallographic data on compounds **2**·acetone, **8** and **9** in the form of CIF files. This material is available free of charge via the Internet at http://pubs.acs.org. The CIF files have also been deposited with the Cambridge Crystallographic Data Centre, Dep. No. CCDC 686881, 686882 and 686883, respectively.

IC801268V

(41) Farrugia, L. J. *J. Appl. Crystallogr.* **1999**, *32*, 837.